



**HAL**  
open science

## Clarification of the hard carbon electrochemical (de)lithiation

Justine Zinni, Lucie Speyer, Léo Duchêne, Carolina Saavedra-Rios, Iona Moog,  
Bruno Delobel, Sébastien Cahen

### ► To cite this version:

Justine Zinni, Lucie Speyer, Léo Duchêne, Carolina Saavedra-Rios, Iona Moog, et al.. Clarification of the hard carbon electrochemical (de)lithiation. *Journal of Solid State Chemistry*, 2026, 359, pp.125975. <10.1016/j.jssc.2026.125975>. <hal-05561637v2>

**HAL Id: hal-05561637**

**<https://hal.univ-lorraine.fr/hal-05561637v2>**

Submitted on 26 Mar 2026

HAL is a multi-disciplinary open access archive for the deposit and dissemination of scientific research documents, whether they are published or not. The documents may come from teaching and research institutions in France or abroad, or from public or private research centers.

L'archive ouverte pluridisciplinaire HAL, est destinée au dépôt et à la diffusion de documents scientifiques de niveau recherche, publiés ou non, émanant des établissements d'enseignement et de recherche français ou étrangers, des laboratoires publics ou privés.



Copyright - All rights reserved



## Clarification of the hard carbon electrochemical (de)lithiation

Justine Zinni<sup>a</sup>, Lucie Speyer<sup>a</sup>, Léo Duchêne<sup>b</sup>, Carolina Saavedra-Rios<sup>b</sup>, Iona Moog<sup>b</sup>,  
Bruno Delobel<sup>b</sup>, Sébastien Cahen<sup>a,\*</sup>

<sup>a</sup> Université de Lorraine, CNRS, IJL, F-54000, Nancy, France

<sup>b</sup> Verkor SAS, 38000, Grenoble, France

### ARTICLE INFO

#### Keywords:

Hard carbon  
Lithiation mechanisms  
Li-ion batteries  
Anode  
Application for energy health and environment

### ABSTRACT

Given the strong growth of the global battery demand and the criticality of graphite, diversifying anode materials in Li-ion systems has become increasingly important. In this context, because of numerous favorable properties, hard carbon is positioned as an interesting alternative. However, due to its structural, textural and chemical complexity, its electrochemical lithiation mechanism remains to clarify. In this paper, a review of the various lithiation mechanisms in hard carbon and their impact on the galvanostatic curves extracted from literature is realized. Thanks to a qualitative and quantitative analysis of the literature, the impact of the surface parameters (specific surface area, defects, heteroatoms, porosity), the turbostratic domains features (size, proportion, interlayer distance) and the closed porosity (size, quantity) on the electrochemical lithiation are highlighted. Their beneficial or detrimental role is discussed, even if some uncertainties remain concerning some aspects such as closed porosity. Finally, other key parameters mandatory for the application are discussed (irreversible capacity, lithium plating).

### 1. Introduction

Lithium-ion battery technology is the most widely used for mobile and stationary energy storage applications. Nevertheless, many researchers are working to further improve this technology through replacing or enhancing component materials (cathode or anode materials, electrolyte, separator, casing ...), interfaces [1] and device (BMS, sensor and actuators [2]). Concerning the electroactive materials, huge work has been dedicated to the development of improved cathodes whereas graphite has remained the dominant anode for decades. Indeed, graphite is a carbon material which exhibits a relatively low specific capacity of 372 mAh.g<sup>-1</sup> but kept many advantages (conductivity properties, mass, electrochemical stability, cyclability, low toxicity ...) compared to other intercalation, alloys and conversion materials [3]. Nevertheless, the graphite supply tends to become a main issue regarding economic, politic and environmental perspective. Indeed, 75% of the synthetic graphite production and graphite mining are localized in Asia, and only 10% and 2% respectively in Europe, making it a critical material in terms of supply and strategic importance [4,5]. Synthetic graphite represents 60 to 80% of the graphite used for LIBs and requires a high energy demand for industrial production [6]. Due to its fossil

fuel precursors (petroleum or coal-tar) and to its energy-intensive production process (Acheson process [7]), synthetic graphite contributes to greenhouse gas emissions (5000 g of CO<sub>2</sub> per kg of graphite produced). Moreover, with the constant development of the on-board energy sector, the global battery demand could be multiplied 14-fold by 2030 (from 180 GWh in 2018 to 2600 GWh) [8]. Consequently, a more sustainable negative electrode material should be considered in order to both answer the increasing demand and drawbacks inherent to graphite.

A possible replacement solution is the use of hard carbons (HC). In Na-ion batteries (NIB), graphite cannot be considered as Na<sup>+</sup> electrochemical intercalation into the host leads to a very low specific capacity of about 35 mAh.g<sup>-1</sup>, mainly due to poor interactions between graphite and sodium [9]. Hard carbons are currently considered as the best solution for practical applications, with a specific capacity that can exceed 300 mAh.g<sup>-1</sup> with a growing knowledge concerning their electrochemical sodiation. This increased comprehension leads the battery manufacturers to open the door to HC as alternative anode for Li-ion battery (LIB's). Compared to graphite, the hard carbon elaboration allows a significant energy saving: the energy used could be divided by 2 or 3 thanks to the lower operating temperature, *i.e.* 800-1500 °C for hard

This article is part of a special issue entitled: Intercalation Today published in Journal of Solid State Chemistry.

\* Corresponding author. Institut Jean Lamour - UMR 7198 CNRS-Université de Lorraine, Campus ARTEM - 2 Allée André Guinier, B.P. 50840, 54011, Nancy Cedex, France.

E-mail address: [sebastien.cahen@univ-lorraine.fr](mailto:sebastien.cahen@univ-lorraine.fr) (S. Cahen).

<https://doi.org/10.1016/j.jssc.2026.125975>

Received 13 January 2026; Received in revised form 16 March 2026; Accepted 18 March 2026  
0022-4596/© 20XX

carbons versus 3000 °C for graphite (Fig. 1) [10]. Moreover, hard carbons can be prepared from low-cost, available and abundant biomass precursors, another advantage for sustainable policies.

HC can be obtained from thermosetting precursors (carbohydrates or polyvinylidene dichloride PVDC) derived from biomass or synthetic and natural polymers. These precursors are usually pyrolyzed at high temperatures (from 700 to 1800 °C) and under inert atmosphere, whereas glassy carbons are formed at higher temperatures (Fig. 1) [10]. Regardless of the pyrolysis temperature, even at high temperatures, hard carbons are unable to graphitize and only random stacking of graphene layers are observed at long distance, with higher interlayer distance than in graphite.

Several models have been used in the literature in order to depict the complex structure and texture of hard carbons. HC can be described as non-graphitizable carbon materials made of a random stacking of graphene sheets along the c-axis with a short-range ordering. These sub-nanometric regions are called turbostratic domains with various structural and chemical defects. They can exhibit a wide range of specific surface area. If the latter is high, it is correlated to highly microporous texture (pore size below 20 Å). However, HC with low specific surface area can also be prepared, whose texture can be microporous or not. The structural evolution of hard carbons with temperature treatment can be described by a schematic model that also helps for depicting alkali ions storage in battery technologies. This description is known as the “falling cards” model (Fig. 2) introduced by Xing et al. [11] and completed by Dahn et al., an advanced model of the “house of cards” model from Xue et al. and Liu et al. [12,13]. It describes the development of the porosity together with the turbostratic domains size increase with the temperature [11,14]. Later, Dou et al. specify this model by considering hard carbons as a combination of pseudo-graphitic microcrystallites (turbostratic stacking of graphene layers,  $sp^2$ -hybridized carbons) and of amorphous regions (defects, layer edges,  $sp^3$ -hybridized carbons) [15].

Currently, no strict definition of the hard carbon structure is clearly established in the literature even if some descriptions have been proposed during the last decades (Fig. 3). A first description has been proposed by Warren et al. who defined hard carbons as an arrangement of turbostratic nanodomains randomly oriented [16]. Later, Franklin et al. have completed this description by precising that these domains were linked to each other through amorphous regions [17]. In 1975, a first 3D illustration has been proposed by Ban et al. who described a network of curved and interlaced graphitic nanoribbons [18]. Nevertheless, in this model, the inability for hard carbons to graphitize is not explained as amorphous linking domains previously mentioned by Franklin are not evocated [17]. Using computational modeling,

Townsend et al. suggested to associate hard carbons with a “random schwarzite structure” containing fullerene-like domains in amorphous regions [19]. Then, Harris et al. claimed that hard carbons were composed of an isotropic and 3D structure similar to foam with curved carbon layers with fullerene-like structure forming microporosity. The non-graphitization feature is explained by non-hexagonal polygons in the structure [20]. Ten years later, Terzyk et al. described hard carbon as a complex porous network composed by carbon layers discreetly curved. Carbon layers do not exhibit only a classical “honeycomb” network but are also composed of a random distribution of pentagons and heptagons helping to stabilize the structure against graphitization [21]. Finally, Dou et al. amended this description with vacancies and heteroatom structural defects in the hard carbon structure [15]. Such a picture of hard carbon with curved graphene layers is commonly accepted in literature. So, typical features of HC are an interlayer distance of  $3.7 < d_i < 4.1$  Å, a crystallite size  $L_a < 10$  nm, a chemical composition of  $>80\%$  at. of carbon, a few mesoporosity and a main microporosity, both open and closed.

Due to the complex structure, the de/lithiation of hard carbons is poorly described in literature. Current batteries involve (de)lithiation of anode and cathode through a “rocking-chair” mechanism. At the negative electrode, the graphite lithiation involves lithium intercalation until saturation of all interlayer spaces with the formation of the  $LiC_6$  first stage Graphite Intercalation Compound (GIC), accompanied with a structural rearrangement in a  $A\alpha A\alpha A$  c-axis stacking sequence clearly identified. So, it is necessary to understand their electrochemical lithiation in the aim of producing alternative batteries with HC as anode instead of graphite. Various approaches such as *ex situ*, *in situ*, *post-mortem* and *operando* techniques [22] can be considered but dissensions emerge from these studies due to the complexity of the materials and the fact that at equilibrium and out-of-equilibrium systems are studied, making conclusions tricky to gather. Hence, the aim of this review is to highlight the keys of the hard carbon electrochemical lithiation, to describe the various lithiation mechanisms suggested in the literature and to assess the possibility to reach a scientific consensus. In this work, all the lithiation modes proposed in the literature are first associated with a respective electrochemical profile. Then, the impact of the main physico-chemical, structural and textural properties is discussed in respect with the evolution of the electrochemical lithiation thanks to a quantitative analysis of data retrieved from the literature. Finally, other factors assumed to be responsible for electrochemical limitations are examined.

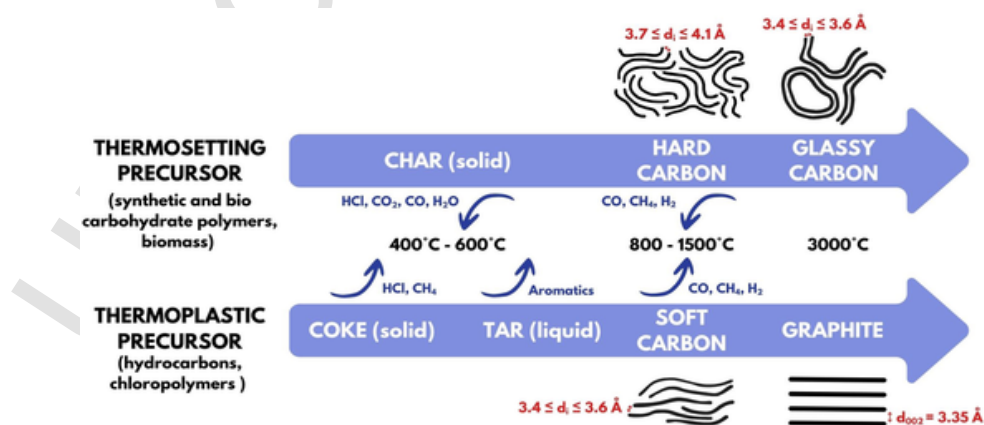


Fig. 1. Schematic representation of carbonization mechanisms for thermosetting (on top) and thermoplastic (on bottom) precursors (adapted from Saurel et al. [10], copyright John Wiley and Sons).

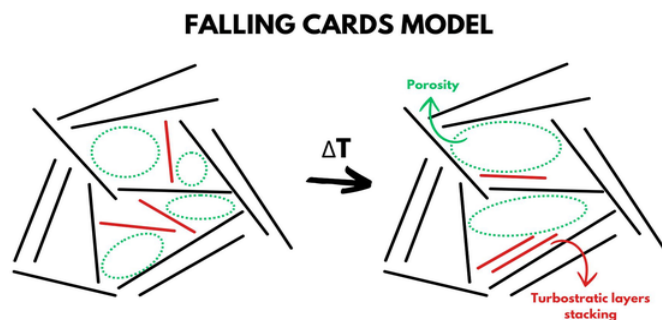


Fig. 2. Schematic illustration of “falling cards” model (adapted from Dahn et al. [14], Copyright (2025), with permission from Elsevier).

## 2. Lithiation mechanisms of hard carbons

### 2.1. Description of supposed mechanisms

As hard carbon sodiation mechanisms are widely studied, a consensus tends to be reached in the literature even if few underlying uncertainties remain. Four mechanisms are identified in literature: pseudo-capacitive adsorption, adsorption on defects, intercalation and pore filling [23,24]. Similarly, some lithium electrochemical insertion mechanisms are admitted while existence of others is still discussed. In the literature, four storage modes are usually described, there are illustrated in Fig. 4

One mechanism is the adsorption phenomena of lithium ions on hard carbon surface, in the surface microporosity and defects forming weak bonds [25]. Lithium adsorption can also occur on the surface of turbostratic microdomains. Kim et al. associate these phenomena with surface adsorption defined as direct reduction of lithium on electrochemically active surface, such as open porosity at the extreme surface of particles [26]. In another step, lithium intercalates into interlayer spaces of turbostratic domains, progressing from the formation of high stage compounds (all spaces are not occupied) to first stage compounds. Intercalation of lithium ions occurs when 2 or 3 carbon layers are stacked [11,27–29]. However, due to the turbostratic nature of hard

carbons, no subsequent stable  $A\alpha A\alpha A$  stacking sequence is possible, which reduces the number of available sites for lithium intercalation [25].

Next, “bulk adsorption” which refers to lithium adsorption in the bulk of hard carbon particles can take place. It occurs at the surface of the so-called closed porosity accessible only to Li ions, and of the ultra-microporosity littering turbostratic domains [14,26,30,31].

Finally, clustering can occur, corresponding to the lithium accumulation in the closed porosity after saturation of the pore walls. There, the state of lithium is not clarified and ionic, metallic, molecular ( $\text{Li}_2$ ) and covalent nature ( $\text{LiC}_2$ ) have been mentioned in the literature [11,25,27,28].

These mechanisms clearly differ from those of graphite lithiation. In the latter case, lithium-ions intercalate in graphite interlayer spaces, whose sites are all considered equivalent. However, the  $\text{LiC}_6$  GIC seems not to be formed after hard carbon lithiation [32]. Moreover, the disordered structure of hard carbons provides electronic and geometric non-equivalent sites (defects, microporosity and particle edges) compared to graphite, modifying the reactivity of carbon versus lithium [29,32].

Because of the small size of lithium and its ability to intercalate in graphite (unlike sodium) one might expect its electrochemical storage in hard carbon to be more significant. In practice, lithium-ions intercalation in hard carbon is limited and the lithium insertion in the porosity is lower than that observed for sodium (Fig. 5) [26].

Finally, every established lithiation mode influences the electrochemical performances and charge/discharge profiles of hard carbons. Several studies have attempted to attribute a mechanism with a lithiation/delithiation step on the typical galvanostatic curves, to ensure safe and efficient batteries.

### 2.2. Electrochemical attribution of the lithiation modes

During electrochemical lithiation of hard carbons, the different lithiation modes previously described are occurring or not, either successively or simultaneously, that explained the discussions in literature. The electrochemical profiles obtained vs.  $\text{Li}^+/\text{Li}$  on hard carbons consist of: a sloping part at high potential (above 0.2 V vs  $\text{Li}^+/\text{Li}$ ) and a plateau part at low potential (below 0.2 V vs  $\text{Li}^+/\text{Li}$ ) [32]. However, the potential delimitation between the two regions is not clearly defined, the plateau is not always identified. In the literature, each section

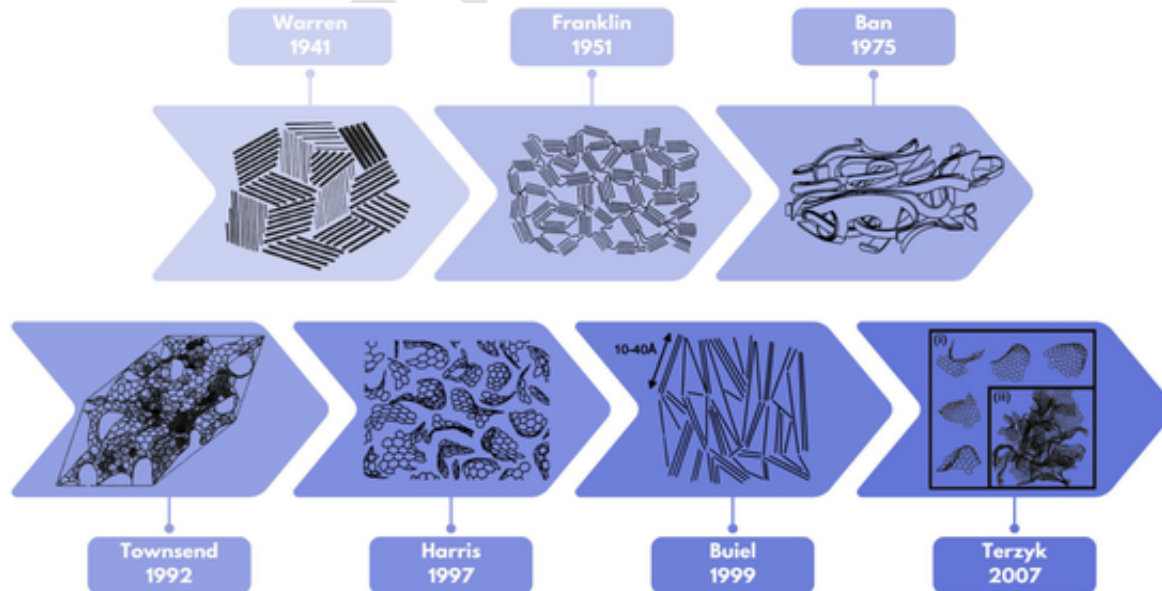


Fig. 3. Evolution of different illustrations and descriptions of hard carbons in literature.

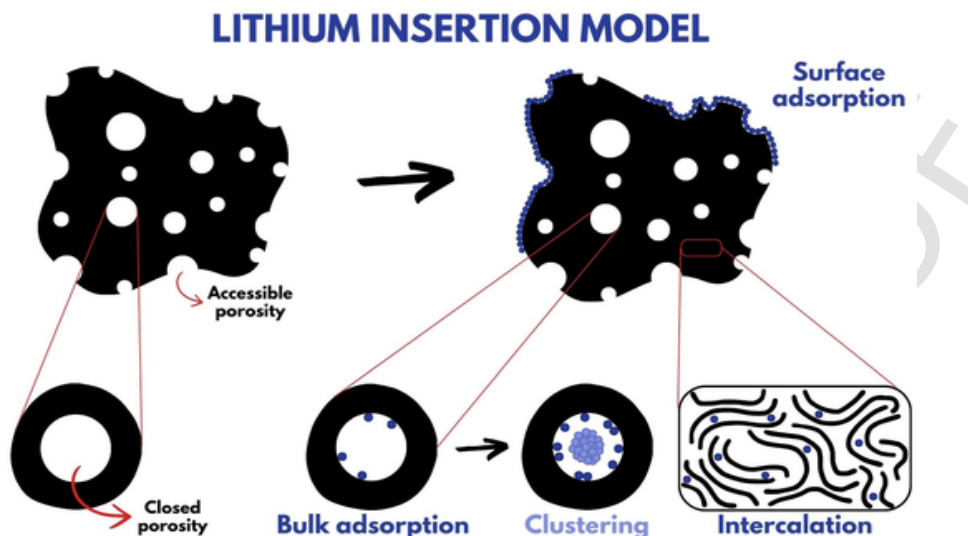


Fig. 4. Schematic illustration of lithium insertion sites in hard carbons.

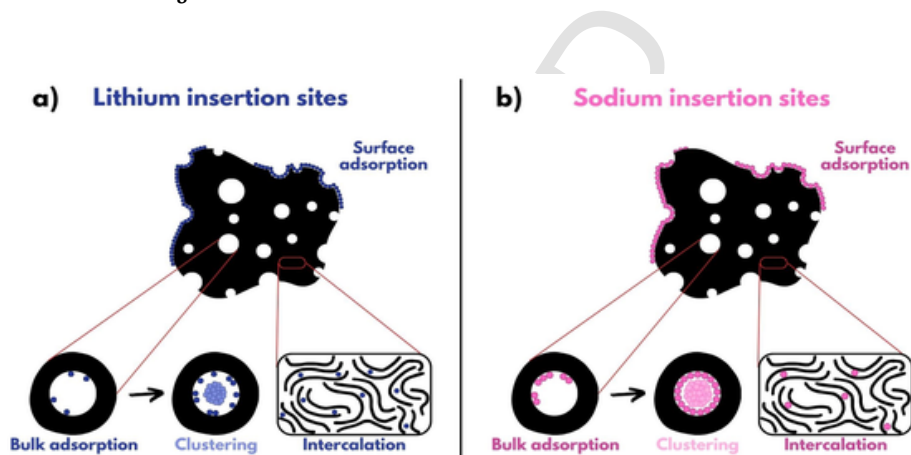


Fig. 5. Comparison of different insertion sites in hard carbons for a) lithium and b) sodium.

of the curve is generally attributed to one or more discussed lithiation modes, and no scientific consensus on these attributions is reached. The different hypotheses for the correlation between the slope and the plateau part with lithium adsorption, intercalation and/or clustering phenomena in hard carbons are presented in Fig. 6 and described below.

- “Intercalation-adsorption” model:

In this model, the reversible capacity and the slope part at high potential of hard carbons is predominated by the lithium intercalation (Fig. 6a)., A debate remains regarding the plateau at low potential. For Liu et al., it is due to a lithium adsorption on layer surfaces undistinguishable from the lithium pore filling [13]. Xing et al. propose that the plateau part is associated to the  $\text{Li}^+$  ions adsorption on the surface of cylindrical closed pores [11]. By *ex situ* techniques, X Ray Diffraction (XRD) and Nuclear Magnetic Resonance (NMR) result Takami et al. claim that the adsorption of lithium in the closed porosity [33]. For Xue et al., that adsorption mainly occurs rather on the two internal surfaces of isolated graphene layers [12].

- “Intercalation-clustering” model:

Similarly, to the previous model, Buiel et al. indicate, based on gas adsorption and XRD analysis, that the lithium intercalation in turbostratic domains is related to the slope part and the plateau corresponds to lithium clustering in hard carbons porosity (Fig. 6b) [34]. Then, Stevens et al. performed *in situ* XRD and proposed the intercalation of lithium at high potential [27]. By *in situ* Small Angle X-Ray Scattering (SAXS), they attributed the pore filling to the low potential part. For Nagao et al., two types of sites show affinity versus lithium: intercalation sites in the turbostratic domains at the surface and adsorption sites in nanosized closed pores. These authors and others have shown these mechanisms by *ex situ* and *in situ* NMR highlighting iono-covalent Li-C bondings and metallic Li-Li bondings related to lithium intercalation and subsequent clustering [35–39]. Finally, Hori et al. comforted the lithium insertion in turbostratic domains for higher potentials (here above 0.1V) and in nanosized pores as Li semi-metallic clusters below 0.1V by *ex situ* X-Ray Photoelectron Spectrometry (XPS), Hard X-Ray Photoelectron Spectroscopy (HX-PES) and NMR [40]. In agreement with Hori’s work, Aniskevich et al. contribute to this “Intercalation-clustering” model through *in situ* Electrochemical Impedance Spectroscopy (EIS), Raman Spectroscopy and XPS [41].

- “Adsorption-intercalation” model:

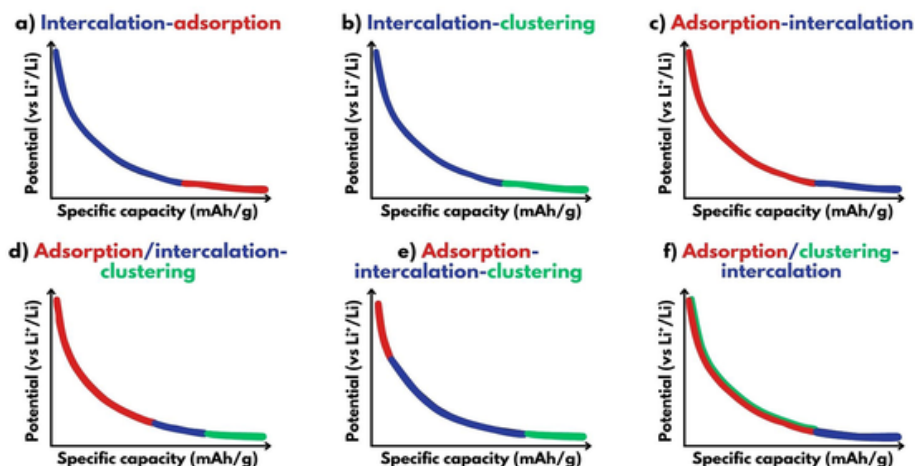


Fig. 6. Different descriptions of the galvanostatic curves with lithium insertion models described in the literature.

Various descriptions of this model are discussed in the literature (Fig. 6c). One reports the existence of a plateau at 0.9 V before the slope part of galvanostatic curves, related to a structural disorder in hard carbon that creates a high surface and pores responsible for new adsorption sites. The plateau part is assigned to the lithium intercalation in hard carbons [42].

More recently and according to other authors, the slope capacity at high potential is related to the lithium adsorption on surface defects and micropores, whereas the plateau capacity is attributed to the lithium intercalation with a reversible expansion-contraction in turbostratic spaces [43,44]. The reversibility of the interlayer distance variation during the lithiation/delithiation was showed thanks to *ex situ* XRD by Liu et al. [44]. Alvin et al. mention that lithium intercalates at 0 V in short vertical distance of turbostratic domains (from 30 to 50 Å along c axis). However, the lithium intercalation is not fulfilled due to turbostratic domains made hardly accessible regarding the tortuosity of hard carbon. Liu et al. demonstrate during the cycling a decrease in the diffusion coefficient at high potential, with an increase at low potential corresponding to the lithium intercalation in turbostratic domains.

Adsorption phenomena occurring in the microporosity up to partial pore filling are also discussed. A correlation is established between the slope capacity and the microporous volume. Finally, the clustering phenomenon is associated with a lithium plating of hard carbons, revealing the difficulty to untangle these phenomena. Notably, Liu et al. show through *ex situ* SEM and XPS analyses that the presence of a long plateau below 0 V can be related to Li-plating as quasi-metallic clusters formed in the volume of nanopores. Intercalation occurs between 0.05 V and 0.1 V, while Li-plating begins below 0.05 V. Due to the proximity in potential, it is likely that these reactions occur simultaneously.

Finally, Saju et al. defend this model by defining the surface lithium adsorption (on the defects, edges and functional groups) in the high potential region and the intercalation in turbostratic domains in the low potential region [29]. Moreover, they explain that a pore filling can take place for hard carbons heated at high temperatures, but this contribution remains low.

- “Adsorption/intercalation-clustering” model:

This model suggests that adsorption and intercalation mechanisms occur in the high potential region.

(Fig. 6d). The slope region is both related to lithium-ions adsorption close to “dangling” bonds and free radical termination, and to a charge transfer between lithium and carbon in turbostratic domains due to in-

tercalation. In this way, the adsorption on the defects is carried out from 2.0 V to 0.25 V, then the intercalation of lithium occurs in an intermediate region (from 0.25 to 0.05 V) and, the quasi-metallic clusters formation in the microporosity happens between 0.05 V and 0.002 V in a plateau zone [45]. This model is also supported by Gotoh et al. whose demonstrate indistinctly by *operando* NMR the signature of intercalated and adsorbed lithium, and the appearance of Li clustering at the end of the discharge [46].

- “Adsorption-intercalation-clustering” model:

Contrarily to the aforementioned model, this one describes the galvanostatic curves in 3 distinct steps (Fig. 6e) [26,47,48]. First, the lithium adsorbs on the surface, then the slope is dominated by intercalation and lastly, the plateau near 0 V corresponds to lithium clustering in the porosity. The two last mechanisms are induced by the surface adsorption, especially the clustering in the closed porosity caused by adsorption of lithium ions on the pore walls (bulk adsorption) until saturation. Manna et al. certify this model with *ex situ* XRD, Raman and XPS experiments, with a dominant contribution of the lithium intercalation in hard carbon [48]. Huang et al. demonstrate the adsorption (3V to 0.2V), the intercalation (0.2V to 0.01V) and the clustering (below 0.01V) of lithium by *in situ* XRD and Raman analyses [47]. Closed porosity and turbostratic domains are related, so as to the relationship between intercalation and bulk adsorption is strong, Kim et al. observed that the more lithium was intercalated, the less it was adsorbed in clusters [26].

- “Adsorption/clustering-intercalation” model:

The last model is supported by Wang et al. (Fig. 6f) [49]. In their work, they attest of the expansion of the hard carbon particles during the lithiation by *in situ* Transmission Electronic Microscopy (TEM). They observe two stages of particle expansion: the first resulting from adsorption phenomena, and the second involving higher expansion with the lithium intercalation into the first stage LiC<sub>6</sub> formation. They assumed the formation of lithium metal nanoparticles at the beginning of lithiation, simultaneously to the surface adsorption phenomena. The authors revealed by the diffusion coefficient analysis, that the capacitive coefficient related to adsorption modes is prominent compared to the diffusion coefficient related to intercalation. The hypothesis of the lithium storage on the surface defects by adsorption and as clusters in the porosity by adsorption at the beginning of lithiation was supported by Issatayev et al. who showed the increase of the specific capacity

from 0.1 to 3 V with the increase of number of defects and porosity in hard carbons [50]. The plateau is associated to the lithium intercalation in turbostratic domains between 0.01 and 1 V.

Finally, in recent studies, a scientific consensus about the adsorption and intercalation storage modes in hard carbons is emerging. Most of the literature agrees with the attribution of the slope region at high potential to the adsorption on the hard carbons surface and, the plateau region at low potential to the intercalation. By contrast, lithium clustering phenomenon and its assignment to the galvanostatic curves is still discussed because the formation of quasi-metallic lithium could be supported with the lithium plating. In this way, the contribution of the *in situ* experiments remains significant issue for the lithiation understanding. However, even if various works dealing with *ex situ* experiments exist and provide initials insights [51], the literature on hard carbon lithiation still lacks *in situ* studies.

### 3. Main characteristics of hard carbons

Each storage mode depends on the different hard carbon properties: chemical composition and surface chemistry, porous texture and structural organization. All these properties are influenced by the elaboration parameters, mainly the thermal treatment temperature of the precursor. It can be first illustrated by the influence of the temperature on first lithiation and delithiation capacities, and on capacity for a given following cycle (Fig. 7) [26,34,43,49,52–68].

Capacities tend to decrease with the elaboration temperature even if some studies report other tendencies such as an overall increase, or an increase only for high temperatures. These observations are representative of the complex interpretations concerning the influence of the hard carbon features on its electrochemical properties. To go further, it is in-

teresting to examine the impact of temperature on slope and plateau capacities (Fig. 8) [26,54,59,60].

Again, even if a general decrease of slope and plateau capacities is observed with temperature, other behaviors can occur. Another electrochemical feature influenced by temperature is ICE (Initial Coulombic Efficiency) (Fig. 9) [53,56,58–61,63–68]. ICE is the ratio between the first charge capacity and the first discharge capacity, and is related to the reversible capacity loss mainly associated to the SEI (Solid Electrolyte Interphase) formation. The latter is formed during the first cycles by electrolyte reduction on the surface of the negative electrode.

Contrary to capacity, ICE is enhanced for higher temperatures. To get a better understanding of these trends, each characteristic of hard carbons will be examined regarding the temperature of elaboration, and the electrochemical behavior.

#### 3.1. Specific surface area and surface defects

The surface control is a key parameter to understand the electrochemical lithiation of hard carbons, especially when the adsorption phenomena are considered as the main lithiation mechanisms. Many surface sites present a specific affinity towards lithium like surface functions, heteroatoms, defects or microporosity.

The influence of temperature on chemical composition (Fig. 10) [59–61,63], structural organization (Fig. 11) [26,43,45,52–57,59–68] and porous texture (Fig. 12) [26,34,43,45,49,52,53,55–64,67,68] is explored.

First, oxygen and hydrogen content decreases with the temperature, which is expected since heteroatoms are progressively eliminated during the precursor pyrolysis. It should be highlighted that the composition also depends on the HC precursor [69].

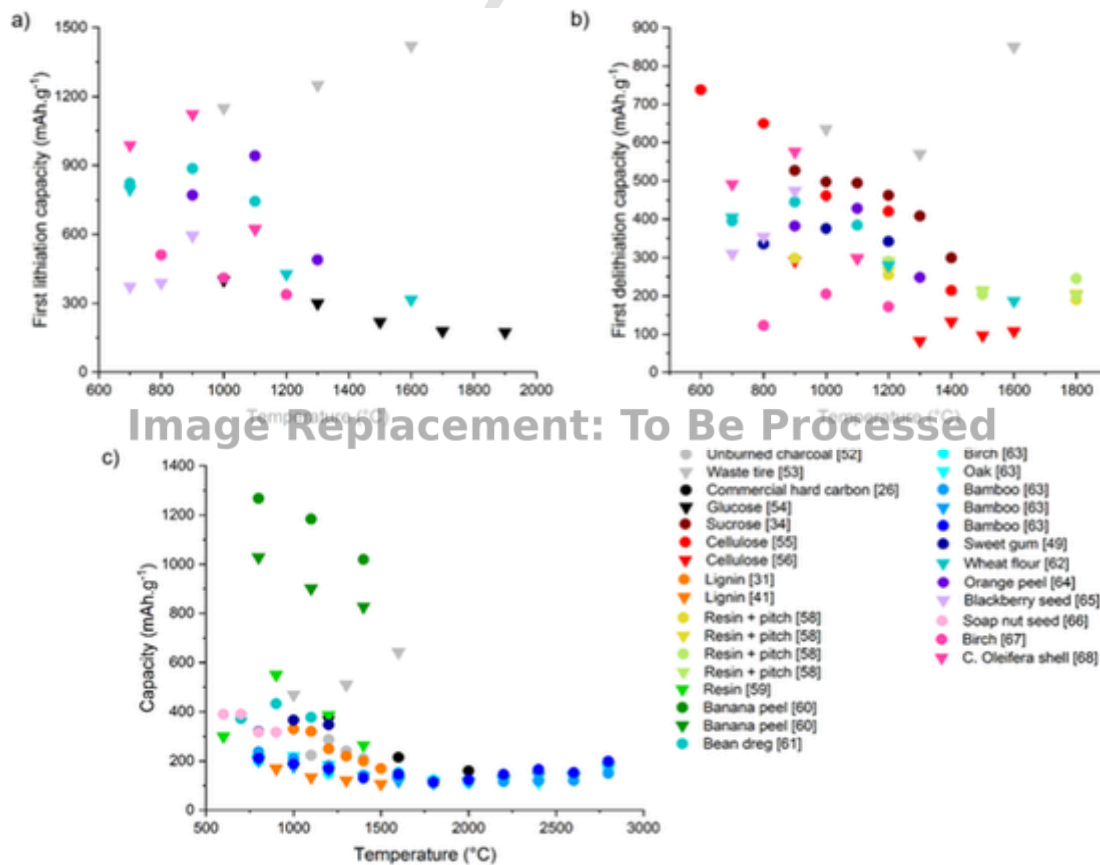


Fig. 7. a) first lithiation capacity b) first delithiation capacity and c) capacity at a following cycle as a function of temperature.

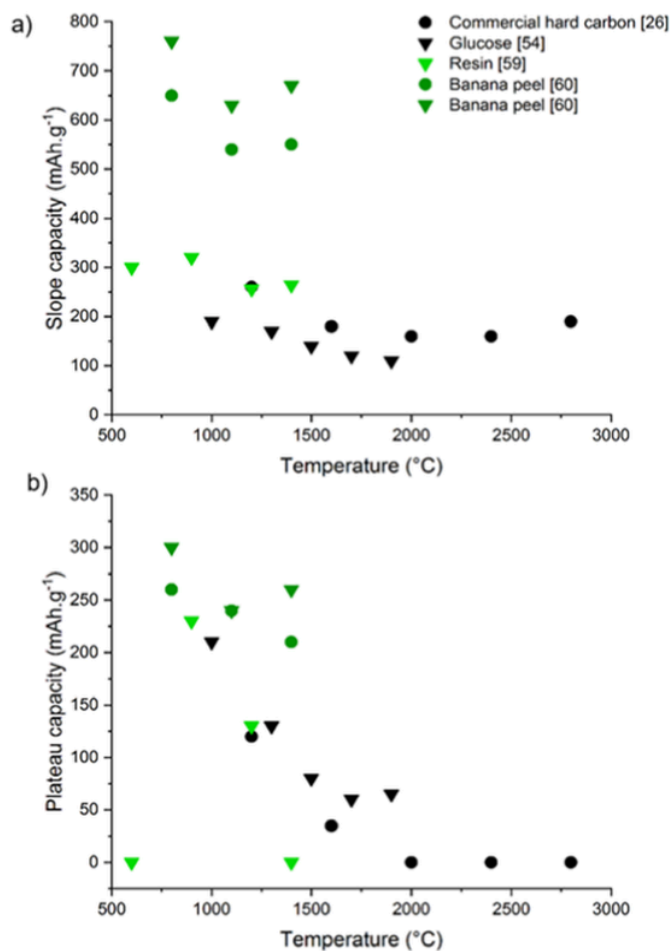


Fig. 8. a) slope capacity and b) plateau capacity as a function of temperature.

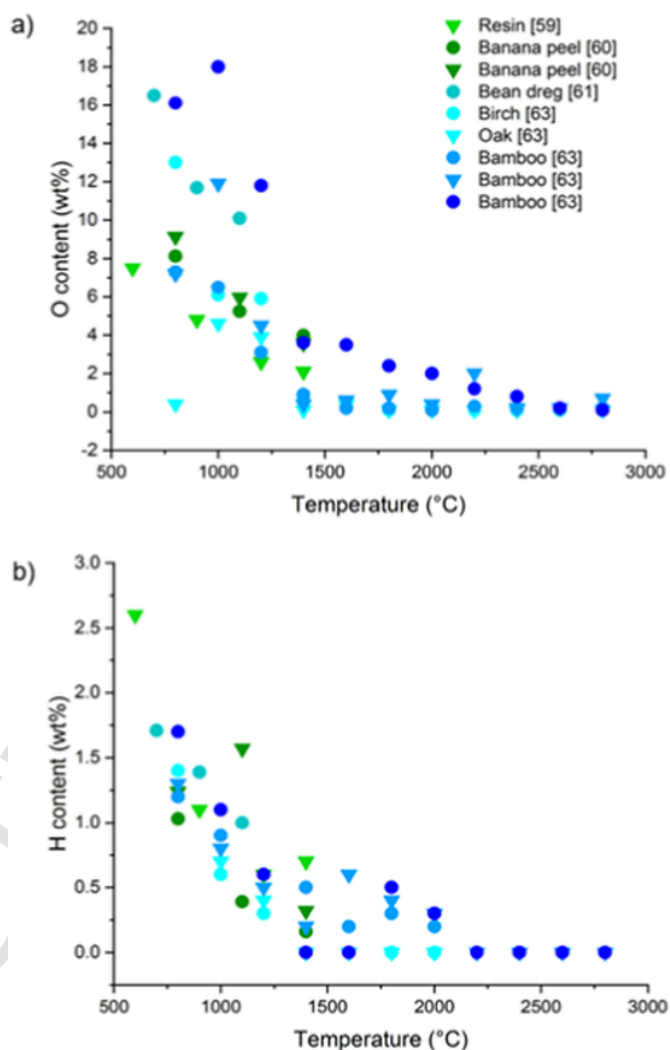


Fig. 10. a) Oxygen and b) hydrogen weight content as a function of temperature.

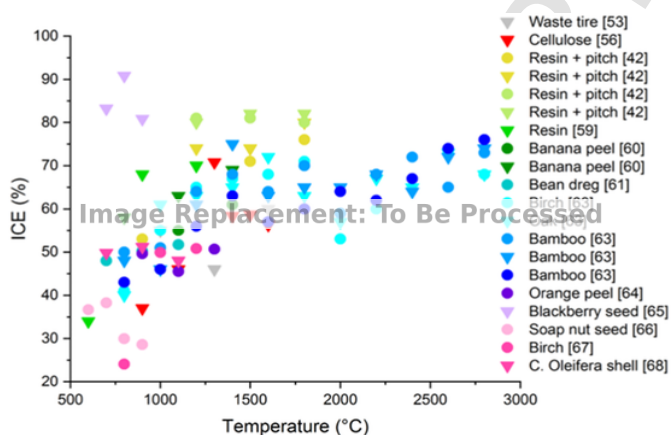


Fig. 9. ICE as a function of temperature.

Concerning the structural organization, crystallite sizes along a and c axis clearly increase with temperature. Even if hard carbons are non-graphitizable carbons, it is however expected that crystalline nanodomains become increasingly developed with temperature, but this evolution is limited compared to soft carbons for example [70].

To evaluate the quantity of structural defects in a carbon material, it is also common to use the  $I_D/I_G$  ratio extracted from Raman spectra, *i.e.* the intensity ratio between the typical D and G bands observed for dis-

ordered carbon materials. If an increase of its value is sometimes reported for low temperatures due to the early development of  $sp^2$  domains at the early stages of graphitization [71],  $I_D/I_G$  value tends to decrease with the development of turbostratic domains with temperature. Both evolutions are observed in literature (Fig. 11).

Finally,  $N_2$  specific surface area decreases when increasing the elaboration temperature. This feature is clearly attributed to the progressive pore closure of hard carbons [17], as first explained by the falling cards model.

### 3.1.1. Heteroatoms

Kubota et al. claim that the irreversible capacity comes from strong interactions of lithium with the surface dangling bonds and the H terminations, causing a plateau at 1.2 V [45]. For Fromm et al., heteroatoms such as hydrogen or oxygen at the surface of hard carbon particles are responsible for lithium trapping [63]. Despite the increase of the stored ions quantity with the development of the terminated hydrogen atoms, hysteresis phenomena between the charge and the discharge were observed. Such observation by these authors is confirmed by the data retrieved from the literature concerning the evolution of ICE with O and H content (Fig. 13) [59–61,63,72,73].

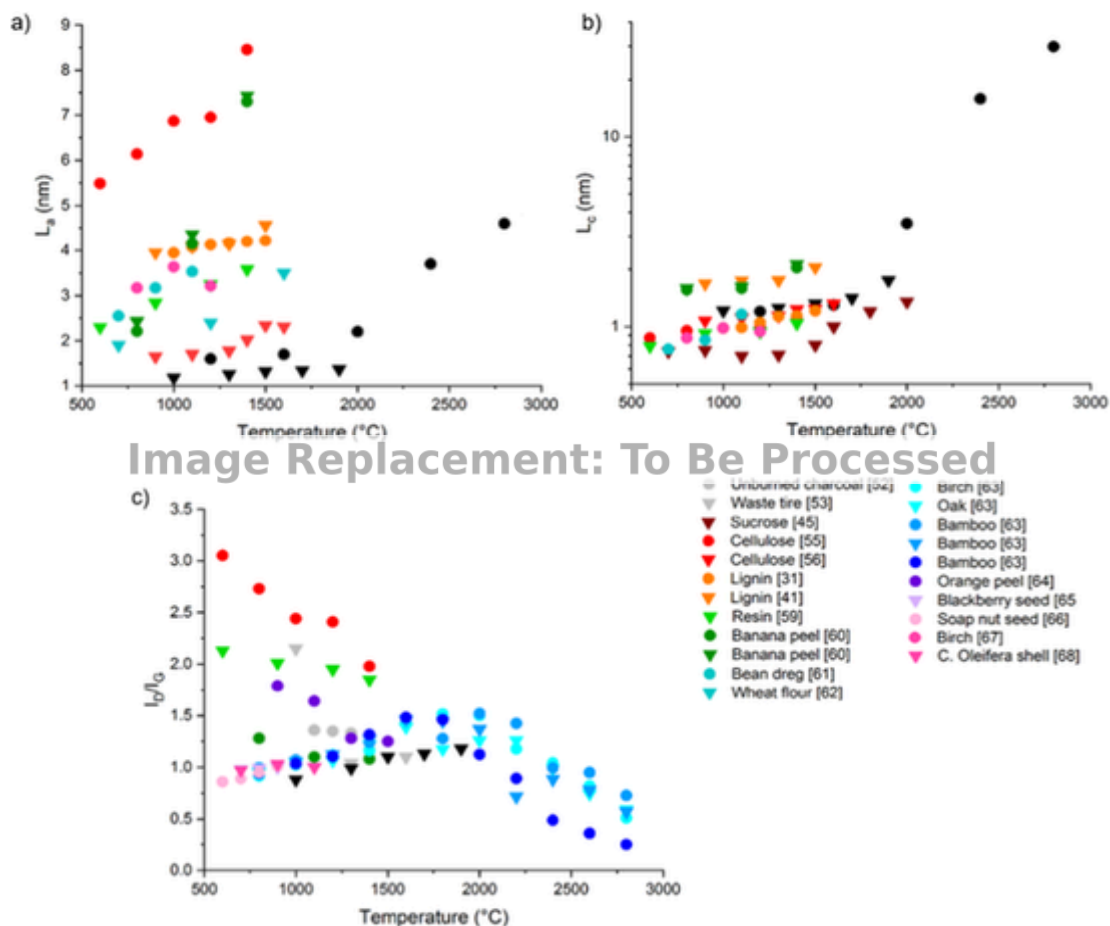


Fig. 11. Crystallite size along a) a axis  $L_a$  b) c axis  $L_c$  and c)  $I_D/I_G$  ratio as a function of temperature.

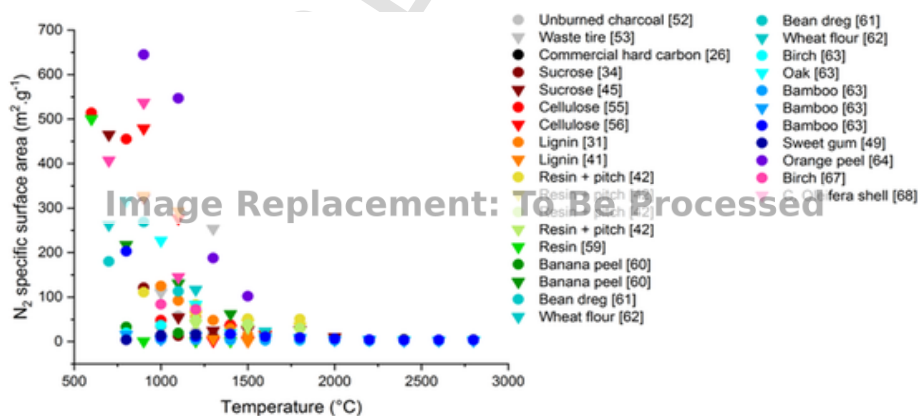


Fig. 12.  $N_2$  specific surface area as a function of temperature.

### 3.1.2. Specific surface area and porosity

Fromm et al. showed a linear relationship between the specific surface area calculated by the BET (Brunauer Emmett Teller) model and the irreversible capacity [63]. For Xing et al., this irreversible capacity increases particularly for the first galvanostatic cycle, and interesting reversible performances are obtained for a specific surface area below  $100 m^2 g^{-1}$  [11,12,74].

A study by Fujimoto et al. demonstrates the appearance of a plateau at low potential and the increase of the reversible capacity with the

hard carbon surface oxidation [75]. The oxidation could modify the geometry of the pore entrance in a way that allows more lithium insertion in pores. Accordingly, Lim et al. claim that the open porosity is necessary for increasing capacity, otherwise its closure induces a reduction of lithium adsorption phenomena [62]. For Liao et al., not only the accessibility but also the micropore volume enrichment would also induces an improvement of the specific capacity [76]. The capacity of various hard carbons (first or other cycles following the authors) are

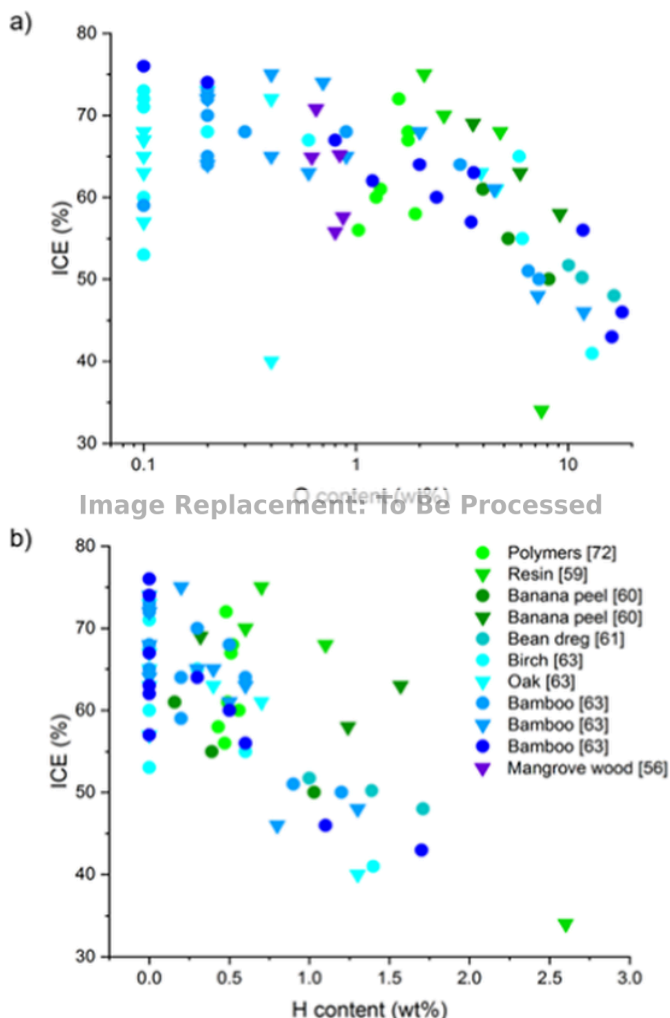


Fig. 13. ICE as a function of a) oxygen and b) hydrogen content.

plotted as a function of specific surface area on Fig. 14 [26,34,43,45,52,53,55–64,67,68,72,77–82].

The absence of a clear trend illustrates the difficulty of bringing conclusions about the influence of porosity, which increases irreversible capacity, but is also described as a promoter for the reversible capacity. Based on a few studies and in an attempt to discriminate the influence of the specific surface area on lithiation phenomena, slope and plateau capacity are plotted separately Fig. 15 [26,59,60,72].

Here, the slope capacity is clearly enhanced when the specific surface area is higher, in accordance with the mechanisms attributing lithium adsorption to this region of the galvanostatic profiles. However, it is not possible to draw conclusions about the plateau.

### 3.1.3. Structural defects

Defects on the  $sp^2$  carbon layers are favored sites for lithium adsorption in wide interlayer spaces in hard carbons [45]. To improve the electrochemical performances of hard carbons for Li-ion, Kubota et al., suggest increasing the quantity of defects, the number of pores and the interlayer distance together with decreasing the specific surface area. Lotfabad et al. investigate the ICE by studying low specific surface area materials which eliminate the effect of the SEI formation [83]. They observe that an ion accumulation during the first cycle, caused by open nanopores filling and adsorption phenomena on defects, cause irreversible lithium-ions intercalation. Especially, surface vacancies are preferential sites for Li due to better thermodynamic stability. How-

ever, the number of surface defects is also addressed to expand the reversible capacity since its ability to improve the capacitive kinetic and to create active adsorption sites [50,54,84]. This idea seems to be confirmed by the development of the capacity between 0.1 and 3 V with the particle grinding [54]. In addition, the surface adsorption would be favored for interlayer spaces large enough, around 20 Å, to contain defect sites considered as redox sites for Li [26]. The electronic affinity of these sites towards lithium induces strong electrostatic interactions between the surface and ions. Finally, the capacity would be increased after successive lithium (de)insertion by creating defects [62]. To explore the impact of defects, Fig. 16 presents the variation of capacity and slope and plateau capacities with  $I_D/I_G$  ratio [26,49,52–55,59,60,62–66,68,78,81,82].

Once again, a clear trend is impossible to establish. It is difficult to distinguish only one trend with the whole capacity, and it is the same when separating slope and plateau regions. It may be because Raman spectroscopy does not probe all kinds of defects that can appear in a material.

To conclude, improving the accessibility and the lithium-ion transport by modifying the specific surface area through the addition of defects, the surface composition and the nanostructured porosity, appears necessary [29]. However, a lower specific surface area improves the ICE and proportionally the irreversible lithium loss but this surface decrease is associated with the decrease of opened porosity which helps to the charge transport and the capacity improvement. A larger quantity of structural defects allows more active adsorption sites and the structural vacancies improve the electronic charge transfer between the surface and lithium. These defects can be added by ball milling, low temperature treatments or varying the elaboration time and atmosphere. Substitution defects such as oxygen and surface dangling bonds also provide energetically favorable sites for adsorption. Doping with heteroatoms (N, P and S) can be considered for modifying the surface electronic properties and for improving the electric conductivity and the Li diffusion coefficient [85–88].

### 3.2. Turbostratic domains

Contrary to the minimal interlayer distance admitted for the sodium intercalation (3.7 Å) in hard carbons for Na-ion batteries (NIB), limited information exists on the effect of turbostratic domains, especially the interlayer distance, on the hard carbon lithiation. However, some considerations are mentioned in the literature. In disordered carbons, the stabilization of the lithium-ions in an  $A\alpha A\alpha A$  c-axis stacking sequence was reported by Dahn et al. [89]. In this study, they suggest that reducing the proportion of turbostratic domains with excessive disorder is important as randomly stacked graphene layers causes a too low density to stabilize the stacking sequence. Furthermore, the spaces are considered as too large to stabilize intercalated lithium in these domains. In Pozio et al. works, the best lithiation material was obtained with the highest graphitization rate which confirms this trend [90]. And, Wang et al. demonstrated that developing the turbostratic domain proportion leads to better electrochemical performances [49]. Contrarily, Chen et al. have recently recommended minimizing the contribution of intercalation into turbostratic domains by controlling their proportion and distribution, favorizing a high disordered structure with large interlayer spaces is assumed to improve other lithiation mechanisms [84]. According to Kubota et al., hard carbons with turbostratic domains separated by small pores are preferable to maximize contact between lithium and carbon layers [45]. Such organization favors the formation of “Li<sub>2</sub>” and “Li<sub>4</sub>” small lithium clusters type to the detriment of weaker lithium-carbon bonds (no LiC<sub>6</sub> compound formation). For these authors, it is necessary to obtain hard carbons with large interlayer spaces for the lithium insertion. Elsewhere, Kim et al. recently proposed another definition for the intercalation in turbostratic domains as the ion storage of lithium by adsorption on the bilateral graphene surfaces

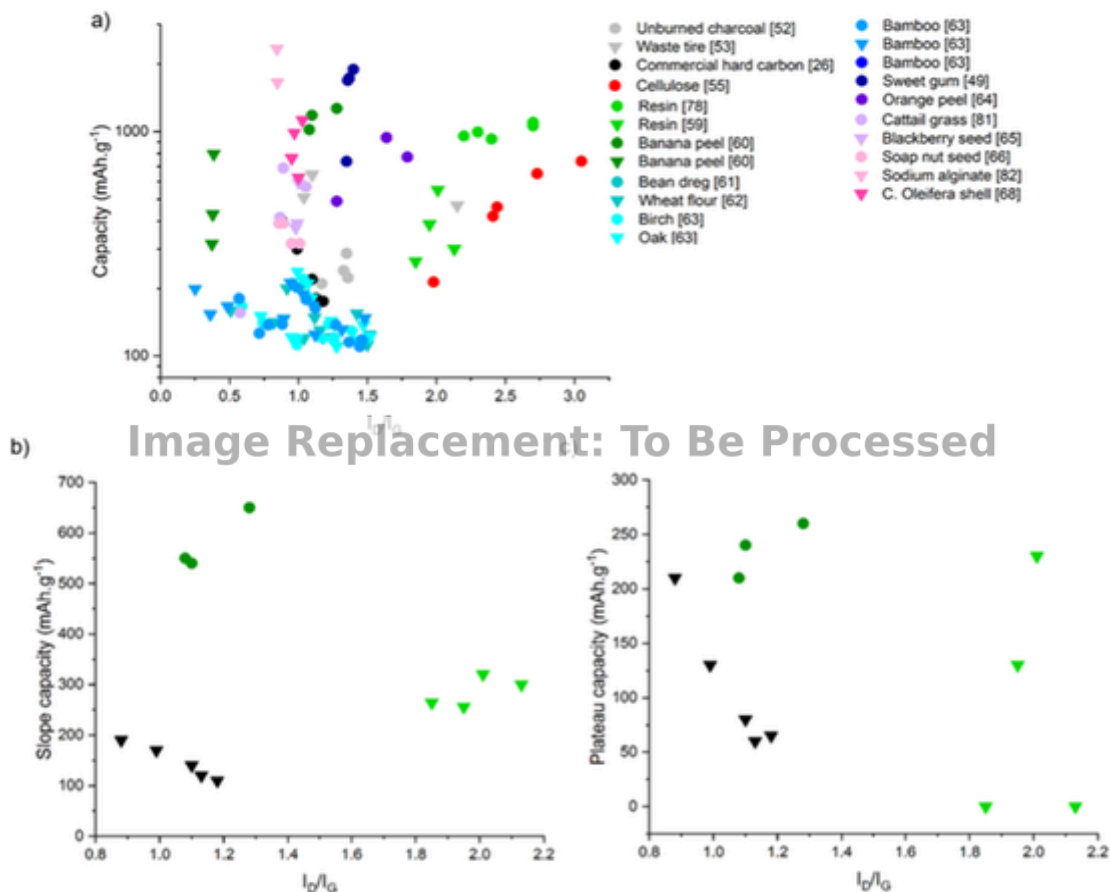


Fig. 14. Capacity as a function of  $N_2$  specific surface area.

(leading to lithium bilayers in the interlayer spaces) or in the closed porosity if the latter exhibits a critical diameter size between 3.6 and 6.0 Å [26]. For these authors, intercalation dominates in the slope part of the galvanostatic curve, especially with interlayer distances below 3.78 Å. That is highlighting the extent to which the debate remains open.

The impact of the interlayer distance on capacities is examined Fig. 17 [26,43,49,52,54–57,59–61,65,67,68,72,73,77–79,81].

Larger interlayer distances globally have a positive impact on the capacity and increase both slope and plateau region.

In contrast, for other authors, the reversible capacity mainly depends on the number of stacked layers which would increase as the c-axis coherence length  $L_c$  increases [13,74], which is not observed by several authors (Fig. 18) [26,43,54–57,59–61,67,77–79].

Finally, the proportion of turbostratic domains needed in hard carbons remains under debate, but the bibliographic analysis leads to some key structural parameters. Small turbostratic domains (along the c-axis) with large interlayer distance seem to provide higher specific capacities.

### 3.3. Closed porosity

Xing et al. observe a relationship between texture and structure: the smaller the pore size is, the higher the proportion of graphene monolayers and the greater the reversible capacity is [74]. For a fixed number of stacked layers, this capacity depends on the aperture, size and surface area of the porosity, controlling lithium adsorption. In correlation with these features of hard carbons, Lim et al. also observe an increase of the reversible capacity when the pore volume increases and the pore size

decreases [62]. For Alvin et al., the optimum of lithiation is obtained when micropores size ranges from 4 to 20 Å [43]. Thanks to modelling, Kim et al. report that bulk adsorption is analogue to the surface adsorption for pore sizes larger than a critical size, also corresponding to a critical interlayer distance [26]. Bulk adsorption occurs for large interlayer distance between 6.0 and 20 Å. For.

Tai et al. also point at the importance of ultramicroporosity for lithium adsorption in the closed pores [59]. In their study, Kubota et al. showed that small microporosity (<10 Å) favors the lithium clusters formation with a formation potential (0.002 to 0.05 V) lower than the graphite intercalation potential (0.09V) [33]. Aniskevich et al. attest the same point of view, because of the pseudo-metallic lithium formation in small clusters, small-sized and narrowed pores are indicated [41]. Here, a consensus seems to be reached with the importance to obtain hard carbon with small pores.

The pore morphology is thus a key parameter for optimizing lithiation, clustering potential and plateau at low potential. The pore closure is responsible for reversible capacity reduction [34], in correlation with a decrease of the lithium-ions adsorption [62]. Some studies claim the ion transport could be easier with a closed macro or mesoporosity, reducing the resistance and creating shorter diffusion paths for lithium [42,50]. Porous carbons offer a specific surface area for adsorption and lithium intercalation sites, and a better stability in the electrolyte because of limited pores-electrolyte interactions.

Note that for Lotfabad et al., pore filling is a partially irreversible phenomenon [83].

To conclude, the closed pore diameter appears as an essential feature and should be at least wider than ionic radius of lithium (0.6 Å) to ensure the lithium-ion storage. Hard carbon with an 3D ordered poros-

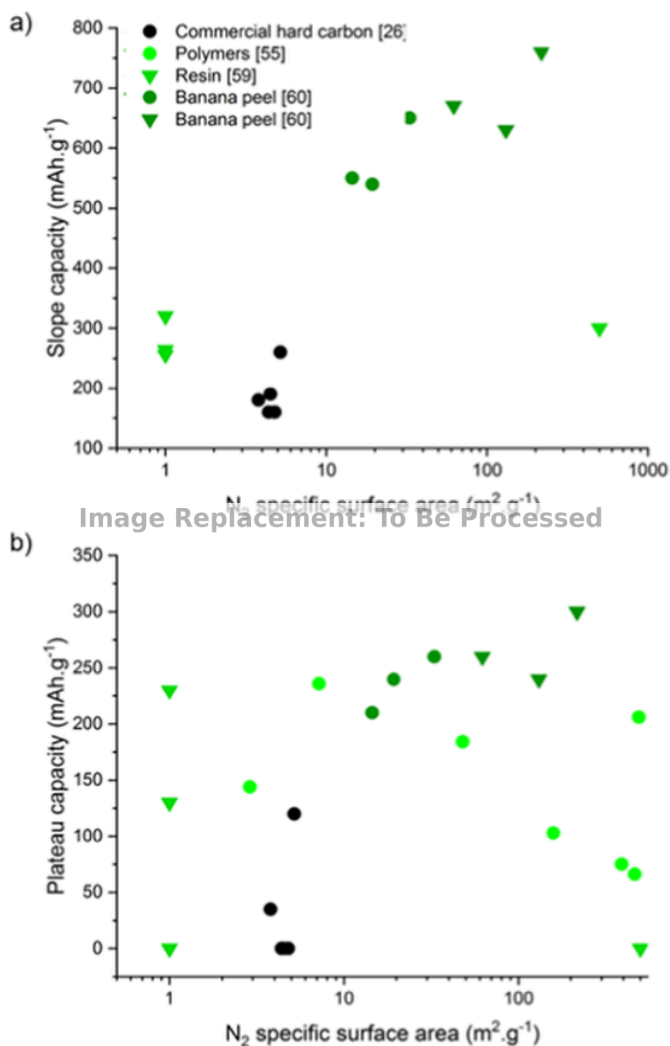


Fig. 15. a) slope and b) plateau capacity as a function of  $N_2$  specific surface area.

ity structure would provide improved electrochemical performances due to enhanced  $Li^+$  ions diffusion phenomena. However, this feature is tricky to obtain and control. In this way, controlling the pore size and distribution is a key parameter for optimizing the storage capacity and the cycle life of hard carbons. Furthermore, the pore closure protects against parasitic interactions with electrolyte which has no longer access to the pore inside. Finally, increasing the closed pore number and size would develop the plateau at low potential [29]. However, compared to Na-ion systems, closed porosity is still poorly studied in the Li-ion literature.

#### 4. Others electrochemical limits

The previous parameters are intrinsic to the material and its elaboration and influence the lithiation mechanisms of hard carbons in various ways. However, other electrochemical limits exist which could be optimized to improve the general hard carbon performances. As the ICE, intrinsically related to the SEI formation, which must be the higher as possible. Lithium plating is also an interesting limitation that could help to develop the reversible capacity of a hard carbon electrode with a controlled dendrite growth.

#### 4.1. SEI formation and ICE

As mentioned before, the SEI results from the reduction reaction of electrolyte on the negative electrode surface area, forming a lithium-ion permeable and protecting passivation layer on the hard carbon surface. The SEI formation is responsible for the irreversibility of the capacity observed at the first cycle, as lithium-ions are irretrievably trapped as various organic and inorganic compounds. In hard carbons, the SEI formation mainly occurs during the first cycle in the potential range of 1 V to 0.8 V, continues to be formed during the first cycles of the battery life and is responsible for the first cycle quasi-plateau at 0.75 V [49,62,91]. The passivation layer mostly consists of hydrocarbons, organic carbonates and lithium salts [40].

ICE is strongly related to SEI, so the SEI optimization is a key parameter for improving the electrochemical performance of hard carbons. It should be noted that an excessive formation of this passivation layer during the first cycle is not only detrimental for performance but also increases the polarization and leads to an important expansion of the electrode volume, which needs to be considered for an accumulator design. Additionally, the extra cathode material needed to compensate for the loss of lithium in a full cell constitute an expensive cost.

Recent studies claim that a low ICE is caused by the irreversibility of the pore filling and surface defects lithiation [32,84]. The first cycle hysteresis would be proportional to the hydrogen amount at the hard carbon surface, inducing a higher lithium deinsertion potential than the insertion one (between 1 and 2 V) [25,62]. The irreversible capacity also seems to be related to the oxygen amount that affects the electrolyte decomposition [63]. Wang et al. show the formation of  $Li_2O$  after the contact between hard carbon and electrolyte [49].

For Buiel et al., two lithium trapping modes responsible for the irreversible capacity coexist: about  $50 mAh \cdot g^{-1}$  related to the SEI formation and around  $150 mAh \cdot g^{-1}$  related to the  $Li_2O$  formation from interactions of lithium with physisorbed water and surface functions [34].

Eventually, decreasing the specific surface area reduces the SEI formation and therefore improves the ICE [32], so a proportionality between the specific surface area and the ICE is proposed [29]. The quantitative analysis of the literature well evidences this correlation (Fig. 19) [53,56,58–61,63,64,67,68,72,77,78,82].

Unfortunately, it is difficult to exceed 80% for ICE, a value remaining particularly low for practical applications [32].

In this way, it was proposed to optimize the closed porosity for developing a lithium-only active surface and for protecting it from interactions with electrolyte. However, the specific surface area must not be neglected and should remain minimal [45].

#### 4.2. Li-plating and dendrites formation

In hard carbon, lithium plating corresponds to the metallic lithium nucleation in micropores only and leads to a decrease of the structural organization [92]. According to the literature, plated lithium in hard carbon has few interactions with electrolyte and associates with defects, inducing the nucleation in this microporosity [32,43,44,92].

After the lithium nucleation as lithium clusters in hard carbon pores, Li-plating occurs uniformly on the surface [44,46]. If Li-plating occurs in excessive quantity, a real risk of dendrite formation exists. By growing, dendrites can pierce through the battery separator and lead to short-circuit with the cathode, causing an uncontrollable thermal runaway. A step and a plateau are electrochemically distinguished below 0 V. The potential of Li-plating was determined between 0 and -0.03 V by several authors [32,43,92]. Below this latter value, the detrimental dendrite formation starts.

However, compared to graphite, where dendrites form needles on the surface (Fig. 20a), the dendrites-electrolyte interaction in hard carbon is minimized due to an internal dendrite growth limiting the electrolyte degradation products (Fig. 20b) [92]. Gotoh et al. precise that

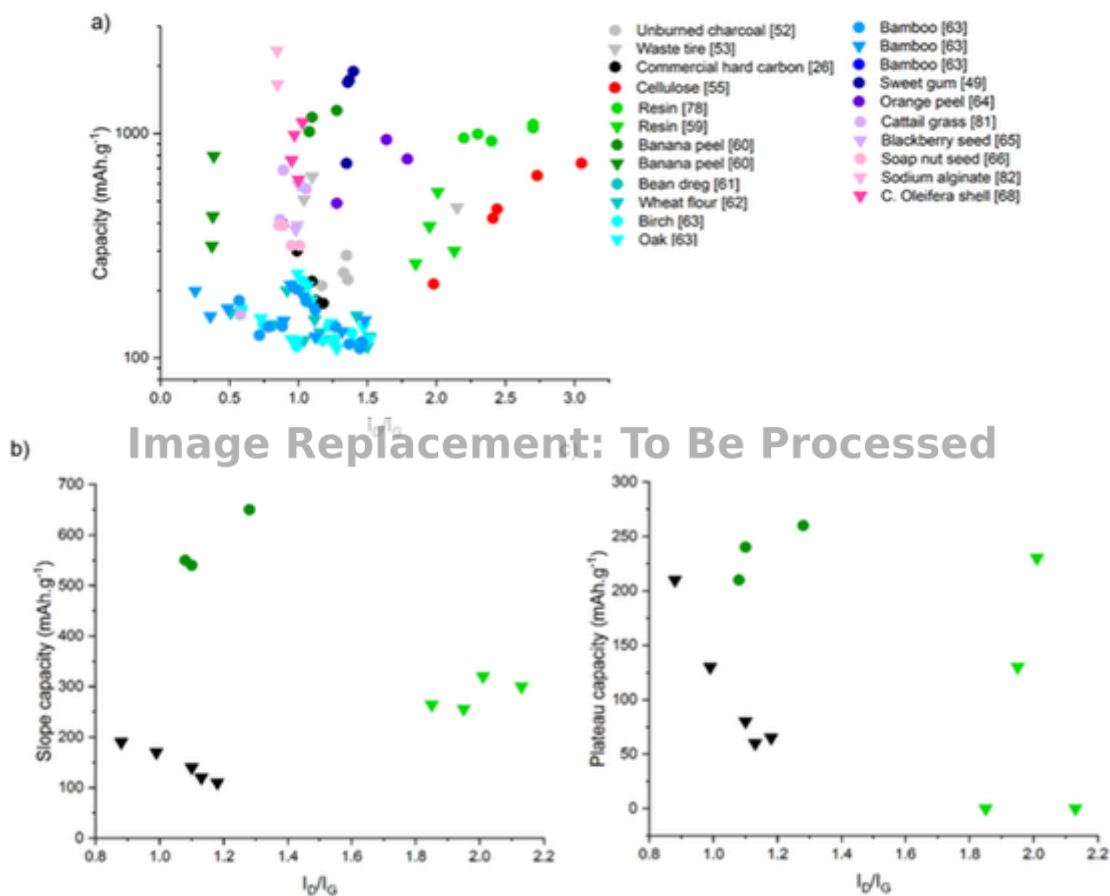


Fig. 16. a) capacity b) plateau capacity and c) slope capacity as a function of  $I_p/I_e$ .

the dendrite growth occurs in the porosity near the surface particle of hard carbon [46].

By taking into consideration these phenomena, broader electrochemical limits can be defined and therefore better performances, since the plateau at low potential can be extended to 0 V without any apparent risk for the battery.

## 5. Conclusion

This review aims to clarify the literature regarding the (de)lithiation behavior of hard carbons for Li-ion batteries applications. Literature is rich in this field of research, so we focused on works published in the last 35 years. In this abundant literature, contradictory studies emerge. We present the different papers in opposition, in the aim to identify common features concerning the electrochemical behavior of hard carbon. First, different interpretations of the electrochemical signature have been proposed by different teams. Moreover, there is still debate in the community concerning the relationship between the complex structural and textural properties of hard carbon in regard with the electrochemical behavior. If the study of papers individually can lead to interpretation that sometimes disagree in between, the strategy developed here is based on a quantitative analysis using experimental data extracted from these papers. Such an approach allows to reveal clearer conclusions to depict electrochemical lithiation of hard carbons. On an applicative point of view, irreversible capacity remains a key point to optimize. The literature also deals with the formation of the SEI, the lithium plating and the dendrite formation and we highlight here some important concepts.

Due to the complexity of the structure, chemistry and texture of hard carbon samples, their properties widely differ from each other. In this way, the experimental protocols of characterization analyses sometimes need to be optimized. From one characterization technique, several ways of data acquisition are possible, leading to different results and interpretations. Thus creates a **no scientific consensus** about the **hard carbon properties** in the community, making the misunderstanding of lithiation phenomena.

Consequently, we resume and describe the four lithiation mechanisms retrieved in the literature, such as **lithium adsorption** on the defects and microporosity of the surface, **bulk adsorption** on the internal closed pores walls, **intercalation** in turbostratic domains and **metal clustering** in the closed porosity of hard carbons. The three first third mechanisms tend to be proven, whereas uncertainties remain for the clustering involvement in hard carbon lithiation. Regarding the galvanostatic profile, two parts are distinguishable: a slope part at high potential and a plateau part at low potential. It is important to note that a long plateau is not systematically observed in the different studies. With this information, the various lithiation modes are successively or simultaneously attributed to one or more potential part, resulting in 6 main models.

Thanks to the **quantitative analysis of the literature**, some conclusions can be drawn. The several studies show a global decrease of the specific capacity with the increase of the carbonization temperature. The same is observed with the slope and the plateau capacities but due to variable galvanostatic profiles, it is difficult to really conclude on this purpose. However, the ICE seems to be improved with the increase of this temperature.

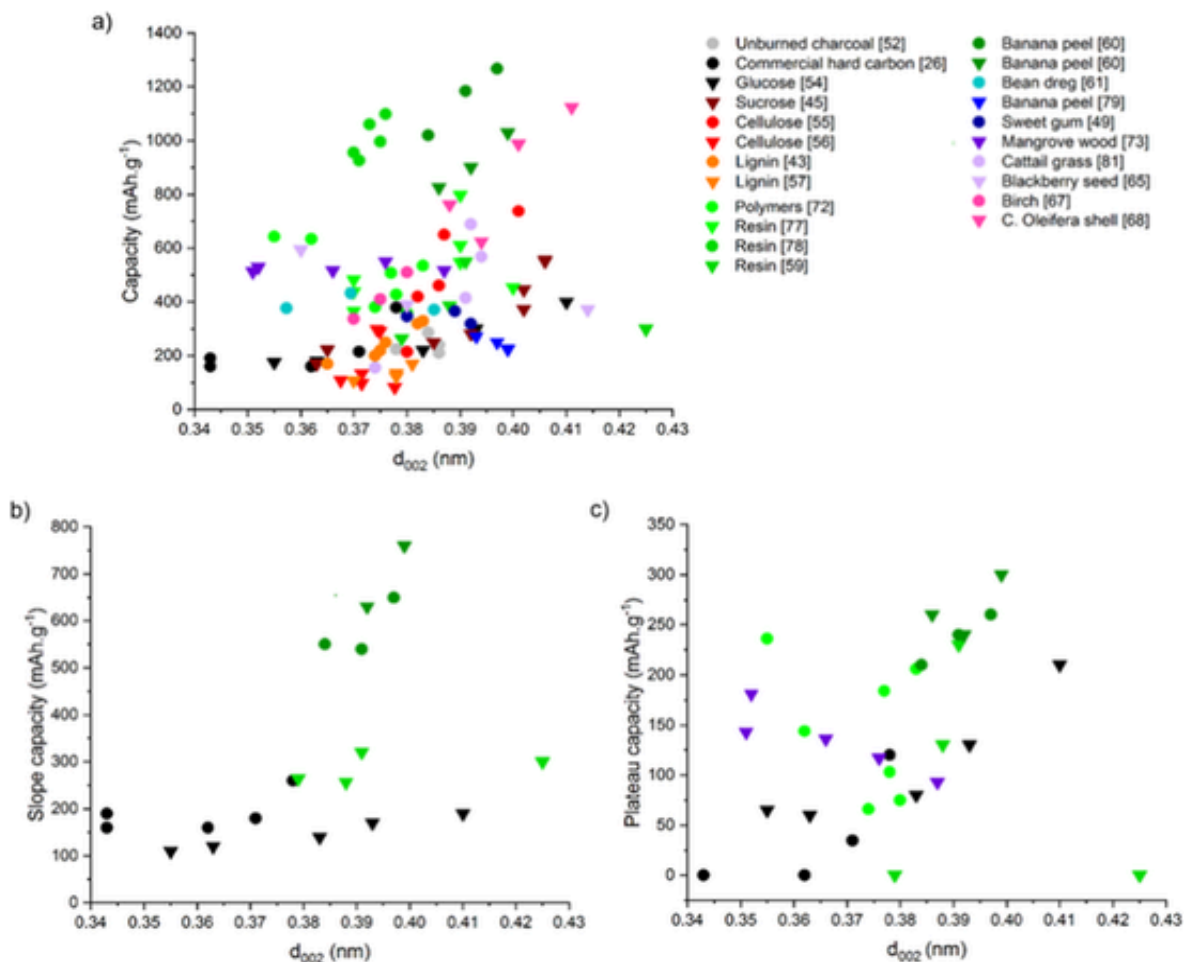


Fig. 17. a) capacity b) slope capacity and c) plateau capacity as a function of the interplanar distance  $d_{002}$ .

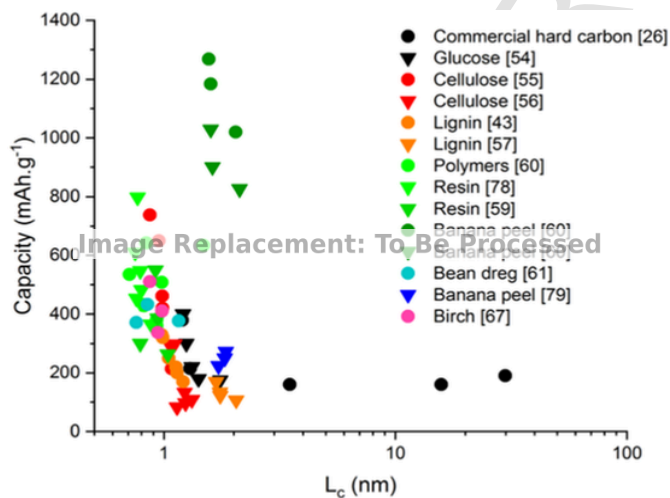


Fig. 18. Capacity as a function of  $L_c$ .

A part of this work is focused on the chemical, textural and structural impact on the lithiation mechanisms. First, the role of the surface and the importance of the surface **heteroatoms**, **specific surface area** and the **surface microporosity** is pointed out. The presence of heteroatoms appears to be detrimental to the reversibility of the capacity

because of their affinity for trapping lithium. A low specific surface area and microporosity would also be beneficial. Nevertheless, all these parameters can be considered as storage sites for lithium, therefore a minimal quantity is necessary, like the slope part that increases with the specific surface area. As well as the diffusion kinetic of lithium ions would be improved by the increase of structural defects quantity.

The most contradictory studies concern the impact of the **turbostratic domains** proportion in hard carbons. Some works report that the quantity of these domains should be maximal when others affirm the opposite. The ideal value of interlayer distance is not defined but larger interlayer spaces tend to improve the capacity, especially the plateau part at low potential. Furthermore, the bibliographic analysis is in favor of small domains, the specific capacity decreases with the  $L_c$  increase.

We highlight that the role of the **closed porosity** is misunderstood and poorly studied. A limited number of studies reveal the importance of the porosity size, and the lithiation improvement would be obtained with a high proportion of small closed pores. The partial irreversibility of the pore filling is also discussed. To go further, an important point to explore is the porosity accessibility regarding the structural organization.

Finally, for Li-ion battery applications, the irreversible capacity is a key parameter to reduce. Two reasons for this irreversibility are mentioned here: the SEI formation that needs to be limited and the presence of chemical, structural and textural defects on the surface of hard carbons. Thus, the higher the surface area, the lower the ICE, the relationship between those two is highlighted here again. For practical issues,

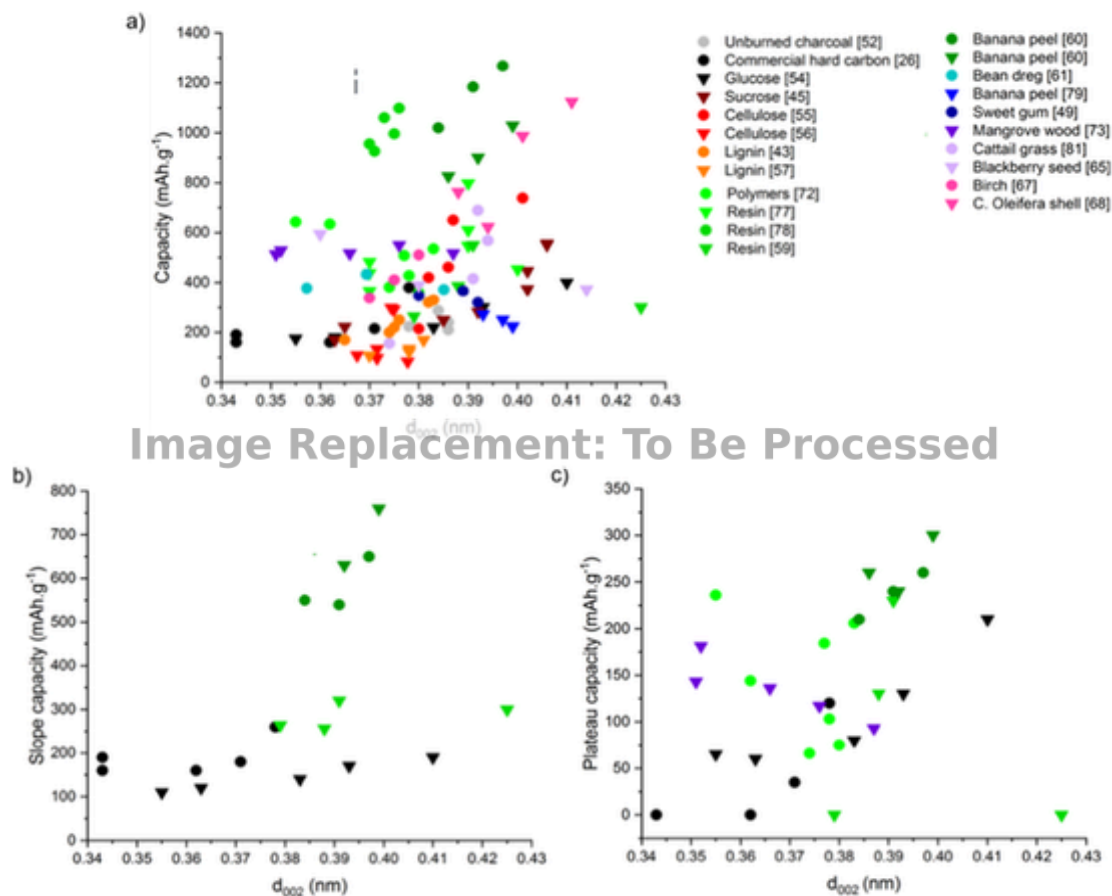


Fig. 19. ICE as a function of N<sub>2</sub> specific surface area.

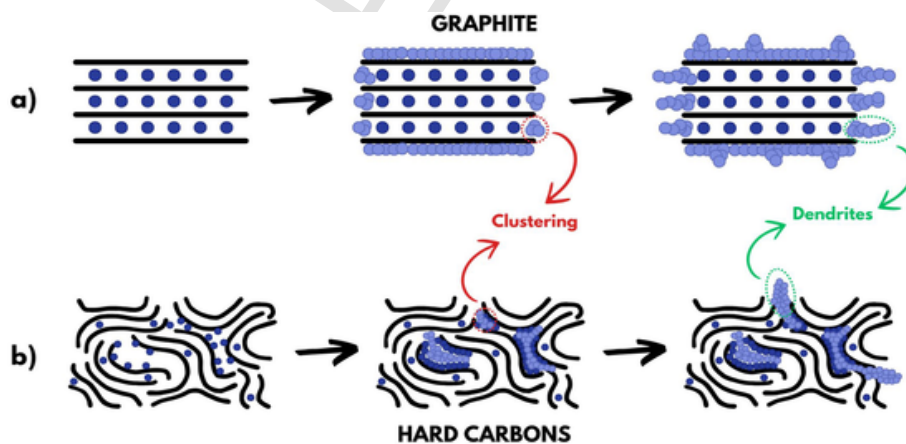


Fig. 20. Schematic illustration of the lithium dendrites formation in a) graphite and in b) hard carbons.

the lithium plating formation is also addressed in this work. It occurs below 0V and becomes detrimental from  $-0.03\text{V}$  by the formation of dendrites. Thanks to the internal formation of this phenomena, additional lithium storage is provided, although irreversible.

Regarding all these points, a predominant issue emerges in this review. The several works presented here cover a wide range of characterization methods including *ex situ* but not sufficiently to overcome the challenges of hard carbons. This is why, *in situ* experiments are posi-

tioned as essential for furthering our understanding of hard carbon lithiation.

#### CRediT authorship contribution statement

**Justine Zinni:** Writing – original draft, Visualization, Methodology, Investigation, Data curation, Conceptualization. **Lucie Speyer:** Writing – review & editing, Supervision, Investigation, Formal analysis, Data curation. **Léo Duchêne:** Writing – review & editing. **Carolina**

**Saavedra-Rios:** Supervision, Project administration, Conceptualization. **Iona Moog:** Supervision, Project administration. **Bruno Delobel:** Supervision, Funding acquisition. **Sébastien Cahen:** Writing – review & editing, Supervision, Funding acquisition.

### Declaration of competing interest

The authors declare the following financial interests/personal relationships which may be considered as potential competing interests: Iona Moog reports financial support was provided by French National Research Agency. If there are other authors, they declare that they have no known competing financial interests or personal relationships that could have appeared to influence the work reported in this paper.

### Acknowledgements

Funding: The authors want to express their acknowledgments to ANRT, France and Verkor company for the financial support (CIFRE convention number 2023/1540).

### Data availability

No data was used for the research described in the article.

### References

- J.-M. Tarascon, M. Armand, Issues and challenges facing rechargeable lithium batteries, *Nature* 414 (2001) 359–367.
- J. Huang, S.T. Boles, J.-M. Tarascon, Sensing as the key to battery lifetime and sustainability, *Nat. Sustain.* 5 (2022) 194–204.
- M.R. Palacin, Recent advances in rechargeable battery materials: a chemist's perspective, *Chem. Soc. Rev.* 38 (2009) 2565–2575.
- BRGM: National geologic service, Géosciences Pour Une Terre Durable, Activity Report, 2020, p. 82.
- Wood Mackenzie, Global Wind Power Market Outlook Update: Q4 2022, 2022 Commodity report.
- S. Bhattacharyya, S. Roy, X. Lin, N. Campagnol, A. Vlad, P.M. Ajayan, Graphite: the new critical mineral, *Nat. Rev. Mater.* 11 (2026) 65–78.
- E.G. Acheson, Process of Making Graphite, 1902 US Patent US711031A.
- Global Battery Alliance, A Vision for a Sustainable Battery Value Chain in 2030, World Economic Forum, 2019, p. 52.
- Y. Liu, B.V. Merinov, W.A. Goddard, Origin of low sodium capacity in graphite and generally weak substrate binding of Na and Mg among alkali and alkaline Earth metals, *Proc. Natl. Acad. Sci. USA* 113 (2016) 3735–3739.
- D. Saurel, B. Orayech, B. Xiao, D. Carriazo, X. Li, T. Rojo, From charge storage mechanism to performance: a roadmap toward high specific energy sodium-ion batteries through carbon Anode optimization, *Adv. Energy Mater.* 8 (2018) 1703268.
- W. Xing, J.S. Xue, T. Zheng, A. Gibaud, J.R. Dahn, Correlation between lithium intercalation capacity and microstructure in hard carbons, *J. Electrochem. Soc.* 143 (1996) 3482–3491.
- J.S. Xue, J.R. Dahn, Dramatic effect of oxidation on lithium insertion in carbons made from epoxy resins, *J. Electrochem. Soc.* 142 (1995) 3668–3677.
- Y. Liu, J.S. Xue, T. Zheng, J.R. Dahn, Mechanism of lithium insertion in hard carbons prepared by pyrolysis of epoxy resins, *Carbon* 34 (1996) 193–200.
- J.R. Dahn, W. Xing, Y. Gao, The “Falling Cards Model” for the structure of microporous carbons, *Carbon* 35 (1997) 825–830.
- X. Dou, I. Hasa, D. Saurel, C. Vaalma, L. Wu, D. Buchholz, D. Bresser, S. Komaba, S. Passerini, Hard carbons for sodium-ion batteries: structure, analysis, sustainability, and electrochemistry, *Mater. Today* 23 (2019) 87–104.
- B.E. Warren, X-Ray diffraction in random layer lattices, *Phys. Rev.* 59 (1941) 693–698.
- R.E. Franklin, Crystallite growth in graphitizing and non-graphitizing carbons, *Proc. Roy. Soc. Lond. A* 209 (1951) 196–218.
- L.L. Ban, D. Crawford, H. Marsh, Lattice-resolution electron microscopy in structural studies of non-graphitizing carbons from Polyvinylidene Chloride (PVDC), *J. Appl. Crystallogr.* 8 (1975) 415–420.
- S.J. Townsend, T.J. Lenosky, D.A. Mulle, C.S. Nichols, V. Elser, Negatively curved graphitic sheet model of amorphous carbon, *Phys. Rev. Lett.* 69 (1992) 921–924.
- P.J.F. Harris, Structure of non-graphitising carbons, *Int. Mater. Rev.* 42 (1997) 206–218.
- A.P. Terzyk, S. Furmaniak, P.J.F. Harris, P.A. Gauden, J. Włoch, P. Kowalczyk, G. Rychlicki, How realistic is the pore size distribution calculated from adsorption isotherms if activated carbon is composed of fullerene-like fragments? *Phys. Chem. Ch.* 9 (2007) 5919–5927.
- V.K. Peterson, M. Bianchini, K.W. Chapman, M. Elice, D.B. Hibbert, P. Roche, L. Silvano, L. Stievano, Terms of Latin origin relating to sample characterization, *Pure Appl. Chem.* 96 (2024) 1531–1540.
- Munnangi R. Anji, M. Helen, A. Groß, M. Fichtner, H. Euchner, Insight into sodium insertion and the storage mechanism in hard carbon, *ACS Energy Lett.* 3 (2018) 2851–2857.
- N. Sun, J. Qiu, B. Xu, Understanding of sodium storage mechanism in hard carbons: ongoing development under debate, *Adv. Energy Mater.* 12 (2022) 2200715.
- M. Winter, J.O. Besenhard, M.E. Spahr, P. Novák, Insertion electrode materials for rechargeable lithium batteries, *Adv. Mater.* 10 (1998) 725–763.
- H. Kim, J.C. Hyun, D. Kim, J.H. Kwak, J.B. Lee, J.H. Moon, J. Choi, H. Lim, S.J. Yang, H.M. Jin, D.J. Ahn, K. Kang, H. Jin, H. Lim, Y.S. Yun, Revisiting lithium- and Sodium-Ion storage in hard carbon anodes, *Adv. Mater.* 35 (2023) 2209128.
- D.A. Stevens, J.R. Dahn, The mechanisms of lithium and sodium insertion in carbon materials, *J. Electrochem. Soc.* 148 (2001) A803.
- K. Sato, M. Noguchi, A. Demachi, N. Oki, M.A. Endo, Mechanism of lithium storage in disordered carbons, *Science* 264 (1994) 556–558.
- S.K. Saju, S. Chattopadhyay, J. Xu, S. Alhashim, A. Pramanik, P.M. Ajayan, Hard carbon anode for Lithium-, Sodium-, and potassium-ion batteries: advancement and future perspective, *Cell Rep. Phys. Sci.* 5 (2024) 101851.
- C. Bomnier, T.W. Surta, M. Dolgos, X. Ji, New mechanistic insights on Na-Ion storage in nongraphitizable carbon, *Nano Lett.* 15 (2015) 5888–5892.
- L. Monconduit, *Les Batteries Na-Ion*, Sciences Ser, ISTE Editions Ltd, London, 2021.
- L. Xie, C. Tang, Z. Bi, M. Song, Y. Fan, C. Yan, X. Li, F. Su, Q. Zhang, C. Chen, Hard carbon anodes for next-generation li-ion batteries: review and perspective, *Adv. Energy Mater.* 11 (2021) 2101650.
- N. Takami, A. Satoh, T. Ohsaki, M. Kanda, Lithium insertion and extraction for high-capacity disordered carbons with large hysteresis, *Electrochim. Acta* 42 (1997) 2537–2543.
- E. Buiel, J.R. Dahn, Li-Insertion in hard carbon anode materials for Li-Ion batteries, *Electrochim. Acta* 45 (1999) 121–130.
- M. Nagao, C. Pitteloud, T. Kamiyama, T. Otomo, K. Itoh, T. Fukunaga, K. Tatsumi, R. Kanno, Structure characterization and lithiation mechanism of nongraphitized carbon for lithium secondary batteries, *J. Electrochem. Soc.* 153 (2006) A914.
- S. Gautier, F. Leroux, E. Frackowiak, A.M. Faugère, J.-N. Rouzaud, F. Béguin, Influence of the pyrolysis conditions on the nature of lithium inserted in hard carbons, *J. Phys. Chem. A* 105 (2001) 5794–5800.
- J.M. Stratford, P.K. Allan, O. Pecher, P.A. Chater, C.P. Grey, Mechanistic insights into sodium storage in hard carbon anodes using local structure probes, *Chem. Commun.* 52 (2016) 12430–12433.
- M. Letellier, F. Chevallier, C. Clinaud, E. Frackowiak, J.-N. Rouzaud, F. Béguin, M. Morcrette, J.-M. Tarascon, The first In-Situ 7Li nuclear magnetic resonance study of lithium insertion in hard carbon anode materials for Li-ion batteries, *J. Chem. Phys.* 118 (2003) 6038–6045.
- M. Letellier, F. Chevallier, F. Béguin, E. Frackowiak, J.-N. Rouzaud, The first In-Situ 7Li NMR study of the reversible lithium insertion mechanism in disorganised carbons, *J. Phys. Chem. Solid.* 65 (2004) 245–251.
- H. Hori, M. Shikano, H. Kobayashi, S. Koike, H. Sakaebe, Y. Saito, K. Tatsumi, H. Yoshikawa, E. Ikenaga, Analysis of hard carbon for lithium-ion batteries by hard X-Ray Photoelectron spectroscopy, *J. Power Sources* 242 (2013) 844–847.
- Y. Aniskevich, O. Zhanadilov, Y. Kim, Y. Ahn, D. Ahn, S. Komaba, S.T. Myung, Unveiling storage mechanisms in hard carbon anodes through In-Situ conductivity and spectroscopy analysis: contrasting lithium intercalation with sodium clustering, *J. Power Sources* 665 (2026) 239077.
- J. Yang, X. Zhou, J. Li, Y. Zou, J. Tang, Study of nano-porous hard carbons as anode materials for lithium ion batteries, *Mater. Chem. Phys.* 135 (2012) 445–450.
- S. Alvin, H.S. Cahyadi, J. Hwang, W. Chang, S.K. Kwak, J. Kim, Revealing the intercalation mechanisms of lithium, sodium, and potassium in hard carbon, *Adv. Energy Mater.* 10 (2020) 2000283.
- Q. Liu, L. Dai, L. Xie, Z. Yi, M. Song, Y. Fan, G. Sun, F. Su, C.-M. Chen, Utilizing the capacity below 0 V to maximize lithium storage of hard carbon anodes, *Particubology* 83 (2023) 169–177.
- K. Kubota, S. Shimadzu, N. Yabuuchi, S. Tominaka, S. Shiraiishi, M. Abreu-Sepulveda, A. Manivannan, K. Gotoh, M. Fukunishi, M. Dahbi, S. Komaba, Structural analysis of sucrose-derived hard carbon and correlation with the electrochemical properties for lithium, sodium and potassium insertion, *Chem. Mater.* 32 (2020) 2961–2977.
- K. Gotoh, T. Yamakami, I. Nishimura, H. Kometani, H. Ando, K. Hashi, T. Shimizu, H. Ishida, Mechanisms of overcharging of carbon electrodes in lithium-ion/sodium-ion batteries analysed by operando solid-state NMR, *J. Mater. Chem. A* 8 (2020) 14472–14481.
- S. Huang, Z. Li, B. Wang, J. Zhang, Z. Peng, R. Qi, J. Wang, W. Zhao, N-Doping and defective nanographitic domain coupled hard carbon nanoshells for high performance lithium/sodium storage, *Adv. Funct. Mater.* 28 (2018) 1706294.
- S. Manna, R. Billa, S. Puravankara, One anode, three ions: mechanistic distinctions of Li<sup>+</sup>, Na<sup>+</sup> and K<sup>+</sup> storage in commercial hard carbon for alkali-ion batteries, *J. Power Sources* 667 (2026) 239235.
- K. Wang, Y. Xu, H. Wu, R. Yuan, M. Zong, Y. Li, V. Dravid, W. Ai, J. Wu, A hybrid lithium storage mechanism of hard carbon enhances its performance as anodes for lithium-ion batteries, *Carbon* 178 (2021) 443–450.
- N. Issatayev, K. Tassybay, N.-L. Wu, A. Nurpeissova, Z. Bakenov, G. Kalimuldina, LiF modified hard carbon from date seeds as an anode material for enhanced low-temperature lithium-ion batteries, *Carbon* 229 (2024) 119479.
- R. Ding, Y. Huang, G. Li, Q. Liao, T. Wei, Y. Liu, Y. Huang, H. He, Carbon anode materials for rechargeable alkali metal ion batteries and in-situ characterization

- techniques, *Front. Chem.* 8 (2020) 607504.
- [52] H.-Y. Yu, H.-J. Liang, Z.-Y. Gu, Y.-F. Meng, M. Yang, M.-X. Yu, C.-D. Zhao, X.-L. Wu, Waste-to-Wealth: low-cost hard carbon anode derived from unburned charcoal with high capacity and long cycle life for sodium-ion/lithium-ion batteries, *Electrochim. Acta* 361 (2020) 137041.
- [53] T. Veldevi, S. Raghun, R.A. Kalaiivani, A.M. Shanmugaraj, Waste tire derived carbon as potential anode for lithium-ion batteries, *Chemosphere* 288 (2022) 132438.
- [54] J. Guo, S. Liu, M. Yang, S. Li, G. Zhang, H. Liu, Utilization of surface-induced capacitive behavior: a promising strategy to improve low temperature performance of Li-Ion batteries, *Carbon* 192 (2022) 227–233.
- [55] Y. Li, Y. Du, G. Sun, J. Cheng, G. Song, M. Song, F. Su, F. Yang, L. Xie, C. Chen, Self-Standing Hard Carbon Anode Derived from Hyper-Linked Nanocellulose with High Cycling Stability for Lithium-Ion Batteries, 3, *EcoMat*, 2021 e12091.
- [56] H. Jang, I. Hasa, H. Kim, Y. Hwa, Y.-W. Byeon, R. Kostecki, H. Kim, Exploring the storage mechanism of alkali ions in non-graphitic hard carbon anodes, *J. Electrochem. Soc.* 170 (2023) 090538.
- [57] L. Fan, L. Fan, T. Yu, X. Tan, Z. Shi, Hydrothermal synthesis of Lignin-based carbon microspheres as anode material for lithium-ion batteries, *Int. J. Electrochem. Sci.* 15 (2020) 1035–1043.
- [58] J. Wang, J.-L. Liu, Y.-G. Wang, C.-X. Wang, Y.-Y. Xia, Pitch modified hard carbons as negative materials for lithium-ion batteries, *Electrochim. Acta* 74 (2012) 1–7.
- [59] C.-W. Tai, W.-Y. Jao, L.-C. Tseng, P.-C. Wang, A.-P. Tu, C.-C. Hu, Lithium-ion storage mechanism in closed pore-rich hard carbon with ultrahigh extra Plateau capacity, *J. Mater. Chem. A* 11 (2023) 19669–19684.
- [60] E.M. Lotfabad, J. Ding, K. Cui, A. Kohandehghan, W.P. Kalisvaart, M. Hazelton, D. Mitlin, High-density sodium and lithium ion battery anodes from banana peels, *ACS Nano* 8 (2014) 7115–7129.
- [61] H. Ru, K. Xiang, W. Zhou, Y. Zhu, X.S. Zhao, H. Chen, Bean-dreg-derived carbon materials used as superior anode material for lithium-ion batteries, *Electrochim. Acta* 222 (2016) 551–560.
- [62] D.G. Lim, K. Kim, M. Razdan, R. Diaz, S. Osswald, V.G. Pol, Lithium storage in structurally tunable carbon anode derived from sustainable source, *Carbon* 121 (2017) 134–142.
- [63] O. Fromm, A. Heckmann, U.C. Rodehorst, J. Frerichs, D. Becker, M. Winter, T. Placke, Carbons from biomass precursors as anode materials for lithium ion batteries: new insights into carbonization and graphitization behavior and into their correlation to electrochemical performance, *Carbon* 128 (2018) 147–163.
- [64] Y. Gao, S. Piao, C. Jiang, Z. Zou, Navel Orange peel-derived hard carbons as high performance anode materials of Na and Li-Ion batteries, *Diam. Relat. Mater.* 129 (2022) 109329.
- [65] C.S. Bongu, A.S. Khan, M. Arsalan, E.H. Alsharaeh, Blackberry seeds-derived carbon as stable anodes for lithium-ion batteries, *ACS Omega* 9 (2024) 16725–16733.
- [66] S. Khatua, K.R. Achary, Y.B. Rao, K. Sasikumar, A.K. Samal, L.N. Patro, Physicochemical activation of soap-nut seeds-derived hard carbon as a sustainable anode for lithium-ion batteries, *New J. Chem.* 48 (2024) 18277–18290.
- [67] Y. Wang, J. Yang, G. Duan, R. Y. X. Han, C. Zhang, J. Han, Q. Fu, H. Yang, S. He, S. Jiang, The role of carbonization temperature and amorphous components for the design and optimization of wood-based hard carbon thick electrodes in lithium-ion batteries, *Ind. Crops Prod.* 227 (2025) 120764.
- [68] L. Zhu, B. Luo, L. Men, J. Chen, F. Xie, W. Zhang, J. Zhang, Y. Zhou, A green synthesis strategy for Lithium/sodium-ion battery anodes: morphology and structure engineering in biochar to boost comprehensive electrochemical performance, *Green Chem.* 27 (2025) 2078–2091.
- [69] Ghimbeu C. Matei, A. Beda, B. Réty, H. El Marouazi, A. Vizintin, B. Tratnik, L. Simonin, J. Michel, J. Abou-Rjeily, R. Dominko, Review: insights on hard carbon materials for sodium-ion batteries (SIBs): synthesis - properties - performance relationships, *Adv. Energy Mater.* 14 (2024) 2303833.
- [70] F.G. Emmerich, Evolution with heat treatment of crystallinity in carbons, *Carbon* 33 (1995) 1709–1715.
- [71] A.C. Ferrari, J. Robertson, Interpretation of raman spectra of disordered and amorphous carbon, *Phys. Rev. B* 61 (2000) 14095–14107.
- [72] A. Piotrowska, K. Kierzek, P. Rutkowski, J. Machnikowski, Properties and lithium insertion behavior of hard carbons produced by pyrolysis of various polymers at 1000 °C, *J. Anal. Appl. Pyrolysis* 102 (2013) 1–6.
- [73] D. Kang, H.-K. Kim, H.-J. Kim, Y. Han, Preparation of biomass-derived hard carbon with uniform ultramicropores for development of fast charging Li-Ion batteries, *J. Alloys Compd.* 900 (2022) 163420.
- [74] W. Xing, J.S. Xue, J.R. Dahn, Optimizing pyrolysis of sugar carbons for use as anode materials in lithium-ion batteries, *J. Electrochem. Soc.* 143 (1996) 3046–3052.
- [75] H. Fujimoto, K. Tokumitsu, A. Mabuchi, N. Chinnasamy, T. Kasuh, The anode performance of the hard carbon for the lithium ion battery derived from the oxygen-containing aromatic precursors, *J. Power Sources* 195 (2010) 7452–7456.
- [76] Y. Liao, J. Hu, X. Zhou, Porous hard carbon microtubes from renewable cotton as high-performance anode material for lithium-ion batteries, *J. Mater. Sci. Mater. Electron.* 32 (2021) 1631–1640.
- [77] S.M. Jafari, M. Khosravi, M. Mollazadeh, Nanoporous hard carbon microspheres as anode active material of lithium ion battery, *Electrochim. Acta* 203 (2016) 9–20.
- [78] Z. Zhou, Z. Gu, Y. He, D. Peng, C. Bao, H. Liu, Controlling the structure and electrochemical properties of Anode prepared from phenolic resin for Li-Ion batteries, *Int. J. Electrochem. Sci.* 14 (2019) 6976–6985.
- [79] F. Luna-Lama, J. Morales, A. Caballero, Biomass porous carbons derived from banana peel waste as sustainable anodes for lithium-ion batteries, *Materials* 14 (2021) 5995.
- [80] K. Yu, Z. Zhang, J. Liang, C. Liang, Natural biomass-derived porous carbons from buckwheat hulls used as anode for lithium-ion batteries, *Diam. Relat. Mater.* 119 (2021) 108553.
- [81] H. Li, L. Song, D. Huo, Y. Yang, N. Zhang, J. Liang, Cattail-grass-derived porous carbon as high-capacity anode material for Li-Ion batteries, *Molecules* 28 (2023) 4427.
- [82] J. Lian, G. Subburam, S.A. El-Khodary, K. Zhang, B. Zou, J. Wang, C. Wang, J. Ma, X. Wu, Critical role of aromatic C(sp<sup>2</sup>)-H in boosting lithium-ion storage, *J. Am. Chem. Soc.* 146 (2024) 8110–8119.
- [83] E.M. Lotfabad, P. Kalisvaart, A. Kohandehghan, D. Karpuzov, D. Mitlin, Origin of Non-SEI related coulombic efficiency loss in carbons tested against Na and Li, *J. Mater. Chem. A* 2 (2014) 19685–19695.
- [84] Z. Chen, Y. Li, L. Wang, Y. Wang, J. Chai, J. Du, Q. Li, Y. Rui, L. Jiang, B. Tang, A comprehensive review of various carbonaceous materials for anodes in lithium-ion batteries, *Dalton Trans.* 53 (2024) 4900–4921.
- [85] J. Ou, Y. Zhang, L. Chen, H. Yua, D. Xiao, Heteroatom doped porous carbon derived from hair as an anode with high performance for lithium ion batteries, *RSC Adv.* 4 (2014) 63784–63791.
- [86] Y. Qian, S. Jiang, Y. Li, Z. Yi, J. Zhou, T. Li, Y. Han, Y. Wang, J. Tian, N. Lin, Y. Qian, In situ revealing the electroactivity of P-O and P-C bonds in hard carbon for high-capacity and long-life Li/K-Ion batteries, *Adv. Energy Mater.* 9 (2019) 1901676.
- [87] X. Cai, Y. Xu, F. Mo, F. Kong, L. Fan, Y. Tan, G. Zhang, S. Chu, W. Chu, S. Tao, L. Song, Toward highly selective heteroatom dopants in hard carbon with superior lithium storage performance, *ACS Appl. Mater. Interfaces* 15 (2023) 29204–29213.
- [88] J.P. Paraknowitsch, A. Thomas, Doping carbons beyond nitrogen: an overview of advanced heteroatom doped carbons with boron, sulphur and phosphorus for energy applications, *Energy Environ. Sci.* 6 (2013) 2839.
- [89] J.R. Dahn, A.K. Sleight, H. Shi, J.N. Reimers, Q. Zhong, B.M. Way, Dependence of the electrochemical intercalation of lithium in carbons on the crystal structure of the carbon, *Electrochim. Acta* 38 (1993) 1179–1191.
- [90] A. Pozio, M. Di Carli, A. Aurora, M. Falconieri, Seta L. Della, P.P. Proisini, Hard carbons for use as electrodes in Li-S and Li-Ion batteries, *Nanomaterials* 12 (2022) 1349.
- [91] W.E. Tenhaeff, O. Rios, K. More, M.A. McGuire, Highly robust lithium ion battery anodes from lignin: an abundant, renewable, and low-cost material, *Adv. Funct. Mater.* 24 (2014) 86–94.
- [92] X. Su, F. Dogan, J. Ilavsky, V.A. Maroni, D.J. Gosztola, W. Lu, Mechanisms for lithium nucleation and dendrite growth in selected carbon allotropes, *Chem. Mater.* 29 (2017) 6205–6213.